Title
Morphometric Analysis of Maxillary Skeletal Expansion Effects on the Nasal Cavity

Author
Moschik, Christoph Erich

Publication Date
2018

Peer reviewed|Thesis/dissertation

UNIVERSITY OF CALIFORNIA

Los Angeles

Morphometric Analysis of Maxillary Skeletal Expansion Effects on the Nasal Cavity

A thesis submitted in partial satisfaction

of the requirements for the degree

Master of Science in Oral Biology

by

Christoph Erich Moschik

2018

ABSTRACT OF THE THESIS

Morphometric Analysis of Maxillary Skeletal Expansion Effects on the Nasal Cavity

by

Christoph Erich Moschik

Master of Science in Oral Biology

University of California, Los Angeles, 2018

Professor Sotirios Tetradis, Chair

Introduction: The shape, size and volume of the bony nasal cavity is highly influenced by the width of the nasal floor, which is formed by the palatine bone and the palatal processes of the maxilla and can be orthodontically manipulated with the MSE (Maxillary Skeletal Expansion) technique. Current evaluation of changes in this area before and after expansion relay on cross-sectional areas and airflow measurements. However, these techniques are not able to truly point out the extend of bone changes and volume changes of this important structure.

Materials and Method: This retrospective study had a sample of 22 patients distributed in two groups. Group 1 was treated with Hyrax and consisted of 6 growing patients (3 females and 3 males, mean age 12y2mo), group 2 was treated with MSE and consisted

of 16 non-growing patients (10 females and 6 males, mean age 20y7mo) who met inclusion criteria. Analysis of CBCT scans before and after expansion treatment was conducted in OnDemand3D software, with automated superimposition on the cranial base. Three reference planes were established, based on reliably identifiable anatomical landmarks, anterior nasal spine (ANS), posterior nasal spine (PNS) and nasion (N). The distance between ANS and PNS in the AP plane was divided into 4 sections, and the distance between ANS and N was divided into 5 sections, excluding the most superior one. Transverse linear measurements at the resulting cross-points between the vertical and horizontal sections resulted in a total of 32 measurement points along the lateral walls of the nasal cavity.

Results: The MSE group showed overall statistically significant larger movements of the lateral walls of the nasal cavity ($p < 0.05$). The bony structures followed the overall expansion pattern of the maxilla, though bending at the orbital rims and areas of higher bone density occurred.

Conclusion: MSE produces not only larger maxillary skeletal transverse movements, but also shows more expansion effects on the lateral walls of the nasal cavity compared to tooth-borne expansion.

The thesis of Christoph Erich Moschik is approved.

Sanjay M Mallya

Carl A Maida

Won Moon

Sotirios Tetradis, Committee Chair

University of California, Los Angeles

2018

DEDICATION

I dedicate this thesis to my family. A special feeling of gratitude to my loving parents, Elisabeth and Erich, who always encourage me to dream big, work hard and aim for perfection. To my grandparents, who supported me in so many ways of life and always helped me to reflect upon myself.

I wish to thank my committee members, who were more than generous with their expertise and precious time. A special thanks to Dr. Won Moon, for giving me the opportunity to contribute to his lab and conduct this interesting research, for being my mentor and for his countless hours of reflecting, reading, encouraging and joyful conversations, not only about scientific subjects but also life itself. His passion and willingness to provide feedback made the completion of this research an enjoyable experience.

TABLE OF CONTENTS

INTRODUCTION

Rapid palatal expansion describes the idea of widening a narrow upper jaw with a fixed appliance and was first described in 1860 by Angell(1). The technique was seen controversial at first, but eventually treatment protocols were established by Goddard and the use of this appliance in children increased(2). In 1956 Andrew Haas reintroduced the appliance in the US and published on the effects of lowering the mandible, widening of the nasal cavity, increase in arch-width, and bite opening(3).
Haas reported about the effects of RPE on the maxillary complex and stated that it is indicated in cases with real and relative maxillary transverse deficiency, nasal stenosis with mouth breathing and the mature cleft patient (4).

Until today, commonly a Hyrax appliance is used in maxillary constricted cases which consists of two metal plates, connected by a jack-screw and stabilization rods. The appliance is mounted to the dentition and the jackscrew is then turned by the patient. Ideally the midpalatal suture separates and a diastema between the maxillary central incisors appears. Expansion success is strongly correlated to the patient's age and maturity, as the midpalatal suture progressively undergoes remodeling and becomes more inter-digitated, serpentine and rigid (5) the more the patient matures. One study by Melson et. al. reports that three stages of suture maturation can be distinguished. Initially the suture is broad and Y-shaped during the infantile period. Then it becomes longer in the vertical aspect and multiple S-curves develop during the juvenile period. The third stage is during the adolescent period and is represented by a very tortuous,

interdigitated suture (6). In 2013 Angelieri and McNamara reported 5 maturation stages of the suture, which can be determined by means of CBCTs. They distinguished if the suture was visible in the maxillary or palatine bones and if it was of high-density or scalloped.

Maxillary expansion is not a pure separation of two plates, but rather a complex rotational movement of the two halves of the maxilla after the midpalatal suture separates. In the literature(7-10) it has been described that the maxillary halves rotate laterally during the expansion, with the center of rotation being closer to the dorsal part and at the height of the fronto-zygomatic sutures. This results in a V-shaped expansion pattern of the midpalatal suture with more opening in the anterior region and less in the posterior region. Lione estimated that the relationship between the anterior and the posterior opening was 60% (10).

Although expansion is attempted in adult patients with conventional tooth born expanders, the effects are more and more dento-alveolar and less skeletal, with more buccal tipping of the teeth, and thus the less effective skeletal expansion (11). Once skeletal maturity is reached, a tooth-borne appliance is not able to deliver high-enough forces to reliably split the suture anymore, producing higher relapse rates, as well as significant dental side effects, high relapse rates or periodontal problems(12). This means specifically buccal tipping of the dentition, gingival recession, periodontal defects of anchor teeth, buccal root resorption as they get pushed through the buccal cortical plate, fenestration of the buccal cortex by tooth roots, bone bending and asymmetric expansion patterns (12-14).

Studies on the effectiveness of Hyrax expansion by Mohan showed that there is a consistent rate of relapse after the expansion, but no difference in the amount of relapse between mixed and permanent dentition(15). Other studies state that the relapse rate can be anywhere from 33-50% (8).

The complications can be reduced or avoided by surgically releasing the osseous structures that resist the expansion forces(16). Historically it was thought that the midpalatal suture was the area of most resistance to expansion on the craniofacial complex. However, Isaacson & Ingram found that the remaining maxillary articulations become the major sites of resistance and this resistance increases with age (17). In 1976 Bell & Epker demonstrated that major resistance to expansion was not the midpalatal suture, but the zygomaticofrontal, zygomaticotemporal and zygomaticomaxillary sutures(18).

Identification of these areas led to the improvement of surgical assisted rapid palatal expansion (SARPE), which was first reported in 1938 by Brown and consisted of a midpalatal osteotomy followed by tooth-borne expansion treatment(19). This procedure resulted in substantial widening of the apical base of the maxilla and the palatal vault, leaving more space for the tongue and swallowing thus reducing relapse. Additional cuts along the areas of resistance at the piriform aperture (anterior), the zygomatic buttress (lateral), and the pterygoid junction (posterior) were emphasized to decrease osseous resistance to the expansion and thus allow a successful expansion(18). More

recently, a paradigm shift to decrease postsurgical morbidity and to allow ambulatory surgery, resulted in osteotomies only in the anterior, lateral and median areas (20). Several authors described a successful surgical expansion with a tooth-borne expander without palatal surgery after a lateral osteotomy from the piriform rim to the pterygoid plate was done (21,22). Glassman further stated that uniform palatal expansion can be achieved without osteotomy of the palate or pterygomaxillary fissure(22).

With the advent of orthodontic mini-implants conventional expander were modified to increase their connection to the bone and to decrease dental side effects (23). Several designs of this mini-implant assisted rapid palatal expanders (MARPE) have been proposed in the literature including one so called Maxillary Skeletal Expander (MSE). The MSE differs from the other MARPE expanders in its placement position which is far more posterior and in the emphasis on bi-cortical engagement of the screws, which leads to more stability and a better force delivery to the palate and the maxillary circumferential sutures(24). This is an advantage, because the posterior palate is considered to be more resistant to expansion forces due to the locking effect of the pyramidal processes of the palatal bones into the pterygoid plates of the sphenoid (25). Another difference of this expander compared to other MARPEs is the strength of the mini-implant used, since they have to be inserted into two cortical layers and regular 7 mm sized mini-implants could lead to screw fracture. Wilmes investigated the factors contributing to fracture resistance of mini-implants in-vitro. In this study fourty-one different mini-implants of various manufacturers with a diameter from 1.3 – 2.0 mm were inserted into an acrylic block and torqued by a robot. The torquing moments until

fracture of the screws were measured and Wilmes concluded that mini-implant diameter highly influences the torquing strength that it withstands. It is therefore recommended to use mini-implants of a higher diameter. Furthermore if a dense bone is anticipated, pilot holes should be drilled (26).

It is well known that bone density not only varies between individuals, but also along the maxillary bone itself. Ludwig evaluated anatomical guidelines for mini-implant placement on the palate by establishing a grid with 16 points and measuring the bone thickness at each position on CBCT scans (27). This proved to be accurate and he concluded that regions of most stable mini-implant placement are the anterior palate and the area 3 mm paramedian to the midpalatal suture(27). Additionally a thin palatal gingiva is considered advantageous for a successful insertion and stability of the screws, as it allows for the abutment head to be closer to the cortical plate and reduces the lever for any force exerted on the screw-head(28).

Current research by Cantarella et. al. demonstrated that skeletally anchored expansion leads to increased widening of the naso-maxillary complex. He showed that the two maxillary halves rotate outwards around a center of rotation slightly above the fronto-zygomatic suture. At the same time this very same rotation results in a slight downward movement of both maxillary palatine processes(29). Furthermore, while the expansion pattern of the midpalatal suture is mostly V-shaped in Hyrax expansions (8,10), it is more parallel with the MSE expander with the same amount of expansion at ANS and PNS. In general, the amount of bone movement is larger with MSE when compared to the Hyrax literature(29).

Considering the anatomy of the nasal cavity, it becomes apparent that the lateral walls are part of the maxilla and will move with it as it expands. One can therefore expect significant changes of the nasal cavity walls result from maxillary expansion. This was described by Ribeiro et al., who investigated changes of the nasal cavity after Hyrax expansion on CBCT. He concluded that there is a significant transverse increase in the lower third, in the anterior, medium and posterior regions. Nevertheless, the expansion pattern of the nasal cavity did not completely follow the V-shaped pattern of the midpalatal suture and the largest increase in transverse width was found in the transverse middle region (30). A more detailed evaluation of the effects of rapid maxillary expansion on the nasal cavity by Palaisa et. al. established three cross-sections with 4mm distance between them and outlines the area change in each of these sections before and after expansion. An average of 25% area increase is reported after a retention period of 3-month post expansion (31). However, this paper does not describe how each of the sections was affected by the expansion nor does it give insight in the pattern of how the nasal cavity changes.

The finding of an increase in nasal cavity size after expansion has been confirmed by Garrett who stated that the lower third of the nasal cavity increases significantly in transverse dimension after rapid maxillary expansion with a Hyrax expander (9). Similar results were reported by Garib, who conducted a study on the effects of maxillary expansion on the maxillary complex and the nasal cavity by means of CT scans. She confirmed the high efficacy of this appliance expanding the palate in the transverse dimension and the reduced expansion effect on the structures of the nasal cavity. Besides measuring the dental arch, he found the smallest transverse increase at the

level of the nasal floor, where the orthopedic effect was one third of the appliance activation(32). No publication on the pattern of expansion of the nasal cavity itself was found in the literature.

Besides the method of measuring the changes of transverse landmarks within the nasal cavity, changes of volumetric measurements on CBCTs are also available in the literature. The nature of these volumetric measurements demonstrates the overall increase in air-volume within the nasal cavity, rather than showing the pattern of expansion in the bony structures. Haralambidis investigated the CBCTs of 24 patients with a mean age of 14.5 years pre- and post- rapid maxillary expansion and calculated the change in volume with Mimics software. He found an average increase of 11.3% in nasal volume, independent from age and sex of the participants (33). This is consistent with other studies, which reported 10.13%(34), 13.8%(35), 17.5%(36), 13.28%(37) of nasal cavity volume increase after expansion with a Hyrax-type expander.

Material & Methods

This study was approved by the Institutional Review Board of UCLA. All subjects included in this study were treated at the UCLA School of Dentistry, section of orthodontics and underwent maxillary expansion as part of their orthodontic treatment. Two different expansion techniques were considered for this study, a tooth-born Hyrax expander and a skeletally fixated MSE (Maxillary Skeletal Expander). This study was retrospective in design and all data were routinely collected as part of the orthodontic treatment. The UCLA orthodontics patient library was searched for patients who met the inclusion criteria of 1) non-growing CVMS IV, 2) maxillary transverse deficiency, 3) treated with either Hyrax or MSE appliance, 4) had CBCT imaging done before and after expansion, 5) visible split of midpalatal suture on CBCT, 6) received no previous orthodontic treatment and 7) had no craniofacial abnormalities.

The group treated with Hyrax consisted of 6 subjects (3 female and 3 males, mean age 12y2mo, age range 9-15) and the MSE group consisted of 16 samples (10 female and 6 males, mean age 20y7mo, age range 17-26).

The Maxillary Skeletal Expander (Biomaterial Korea Inc.) consists of a hexagonal-screw with two attached movable parts with holes for the placement of four mini-screws and is attached to two molar bands. Each activation turn of the hex-screw separates the two moveable parts by 0.16 mm. The expander is fixated to the palate with four mini-screws (Biomaterials Korea Inc.), with a length of 11 mm or 13 mm and a diameter of 1.8 mm that fit tight into the guidance holes (Figure 1).

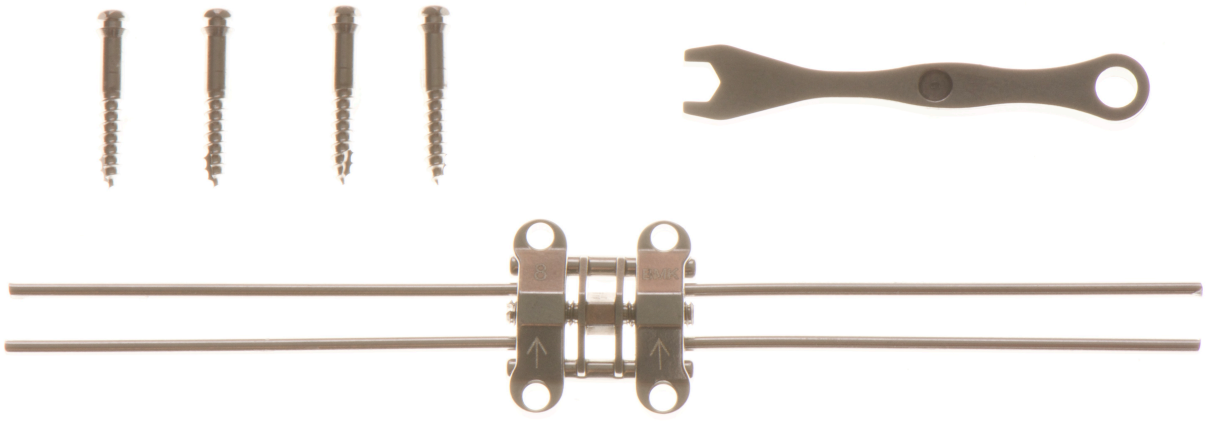

Figure 1: MSE appliance by Biomaterials Korea Inc. Company

The necessary length of the screws for bi-cortical engagement was determined by measuring the thickness of the palatal hard- and soft-tissue on the CBCT. Each appliance was fabricated by sizing molar bands, taking a pick-up impression and pouring it in stone, placing the posterior part of the central body of the appliance 1-2 mm anterior to the junction of the hard and soft palate flush against the palatal vault, fitting the supporting arms to the lateral walls of the palate with 2-3 mm clearance, and soldering the arms to the molar bands. The appliances were then cemented intra-orally, and four mini-screws were placed chairside under local anesthesia (Figure 2a). Patients were instructed to turn the jack-screw four times per day, resulting in 0.6 mm activation.

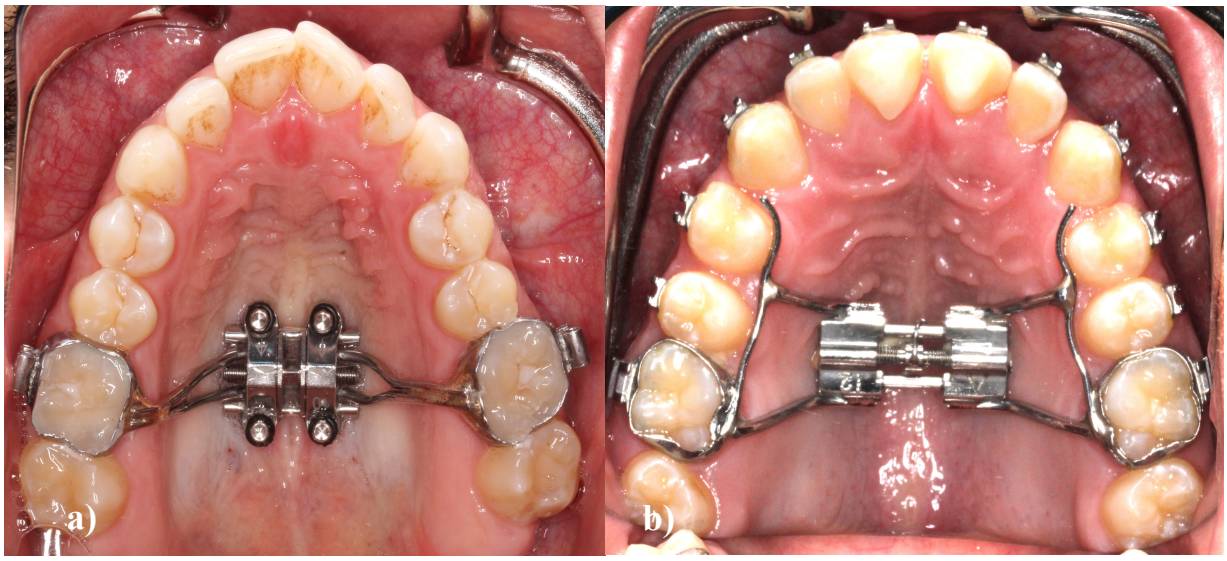

Figure 2: a) MSE appliance in situ **b)** Hyrax appliance in situ

The Hyrax appliance used in this study consisted of a central expansion screw attached to two molar bands on maxillary first molars and lingual bar extensions (Figure 2b). These appliances were fabricated in a similar manner as the MSE appliances and were cemented intra-orally. Patients were instructed to complete one full turn of the expansion screw each day until the WALA ridges lined up and expansion was achieved, with each turn producing 0.25mm of expansion.

CBCT scans were taken both before expansion and right after completion of expansion on all patients. All CBCT scans were taken by a NewTom 5G machine in an 18x16 Field of view with a 14 bit gray scale. Scan times were 18 seconds (3.6 seconds emission time), 110 kV, and utilized an automatic exposure control that adjusted the milliampere based upon the patient's anatomic density. The NewTom 5G Safebeam control reduces the radiation the patient is exposed to, based on the patient's size. Data from the CBCT was reconstructed to produce 0.3mm slices.

Creating CBCT volumes with different spatial orientations

The DICOM files corresponding to the pretreatment CBCT scans of 22 patients (gold standard) were imported into OnDemand3D software (version 1.0.10.5385; Cybermed, Seoul, Korea) and organized in the database management module. Each CBCT volume was opened and saved in the programs library. This procedure was performed for all 22 pre-treatment and post-treatment CBCT volumes, creating 44 CBCT volumes in the program library.

CBCT volume superimposition

For the fully automatic voxel-based rigid registration, the fusion module in OnDemand3D was used. Axial, sagittal, and coronal slice views of the volumes were used to select the anatomical structures of the anterior cranial base in the CBCT volumes. Next, OnDemand3D automated registration tool was used to perform rigid registration (translation and rotation) that optimally aligned the post-treatment CBCT volume to the pre-treatment CBCT volume, using the intensity of the grey levels for each voxel in the anterior cranial base of the two CBCT volumes. The same voxel-based superimposition procedure was used to align pre-treatment and post-treatment CBCT volumes of growing patients subjected to RPE, using the anterior cranial base as reference.

Reference planes and validation

Three reference planes (Figure 3) were constructed which then allowed to measure changes in all three dimensions of space. As a plane is constructed by the means of

three points, it was necessary to use three distinct anatomical landmarks for each plane.

The first points were the anterior nasal spine (ANS), posterior nasal spine (PNS) and the middle of the fronto-nasal suture (Nasion). The resulting plane was called Maxillary-Sagittal-Plane (MSP).

For the second plane only two landmarks were needed. It was constructed through the points ANS-PNS and being perpendicular to the MSP. This plane was called the Horizontal plane.

Like the second plane, the third plane was constructed through two points and being perpendicular to the MSP. The points used were ANS and the middle of the fronto-nasal suture and the resulting plane was called the Coronal Plane.

The planes were constructed on the pre-expansion CBCT volumes and kept for the post-expansion CBCT volumes. This allowed to maintain the same reference plane for the pre- and post- treatment measurements.

Validation of the reproducibility of the planes was calculated following Woller's protocol by repeatedly measuring the distance from the planes to basion, the most outer point of the right anterior clinoid process and the mid-point of the posterior border of sella turcica on 25% of the sample (7). This demonstrated high accuracy with an intra-class correlation coefficient of 95.5% and Cronbach's alpha of 98% respectively.

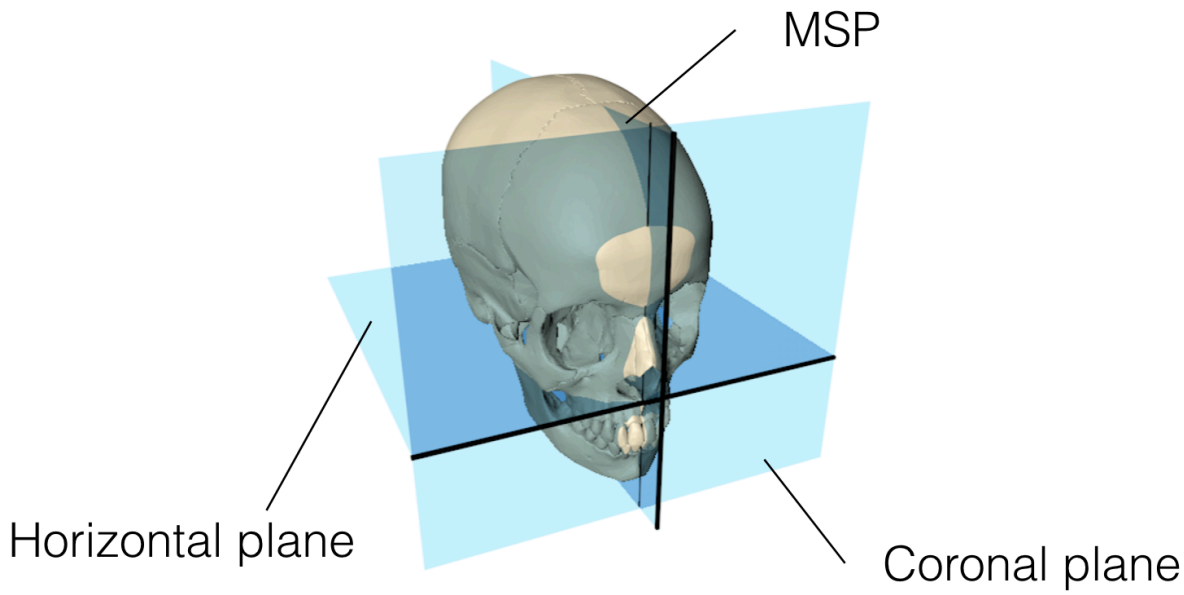

Figure 3: Demonstration of reference planes

ANP / MNP / PNP / TNP

The distance between nasion and PNS was divided by four equally distributed cuts parallel to the coronal plane and perpendicular to the horizontal plane. The planes were then named after the section they describe as 1) Anterior Nasal Plane (ANP), 2) Middle Nasal Plane (MNP), 3) Posterior Nasal Plane (PNP) and 4) Terminal Nasal Plane (TNP), which can be seen in Figure 4. The average distance between these planes was 9.48 mm with a range from 7.70 mm to 11.27 mm.

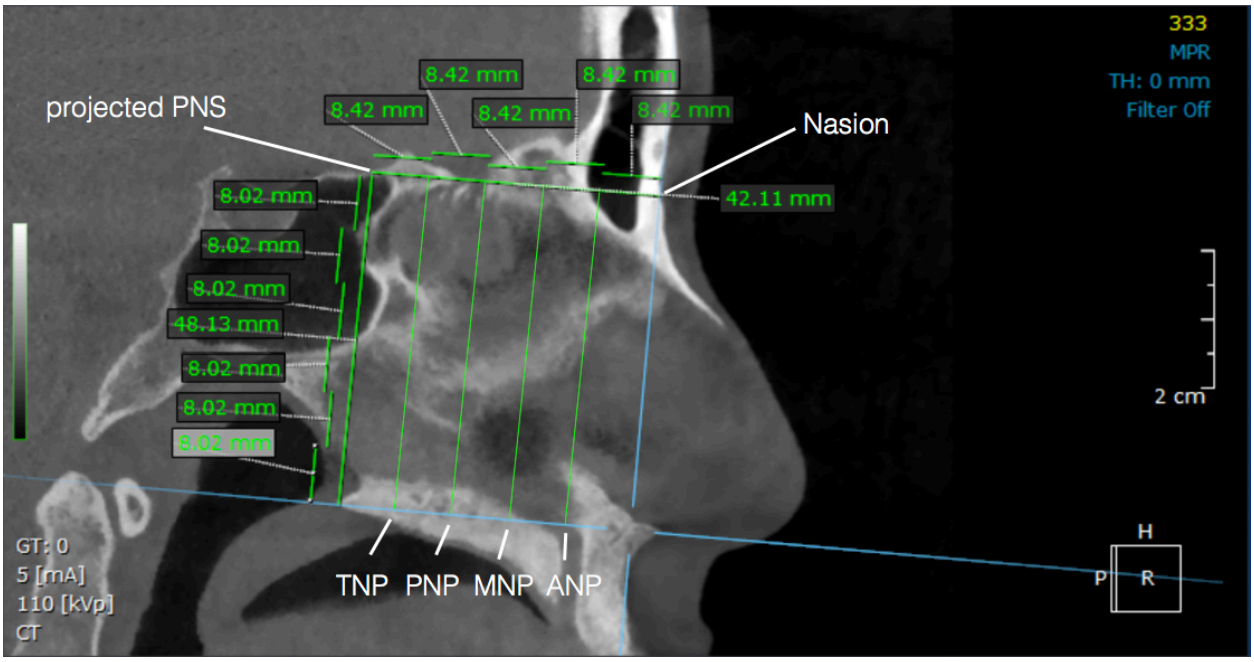

Figure 4: ANP, MNP, PNP and TNP; This figure shows the four cuts between nasion and PNS and their description as ANP, MNP, PNP, and TNP.

ENS, UNS, MNS, LNS

Additional horizontal cross-sections through the nasal cavity where then needed to further divide the nasal cavity into small partitions. Five cuts parallel to the horizontal section where made and equally distributed between nasion and ANS. The most upper section was repeatedly outside of the nasal cavity and therefore excluded from this study. The remaining four sections were 1) Ethmoidal-Nasal-Section (ENS), 2) Upper Nasal Section (UNS), 3) Middle Nasal Section (MNS), 4) Lower Nasal Section (LNS). See Figure 5 for details about these sections.

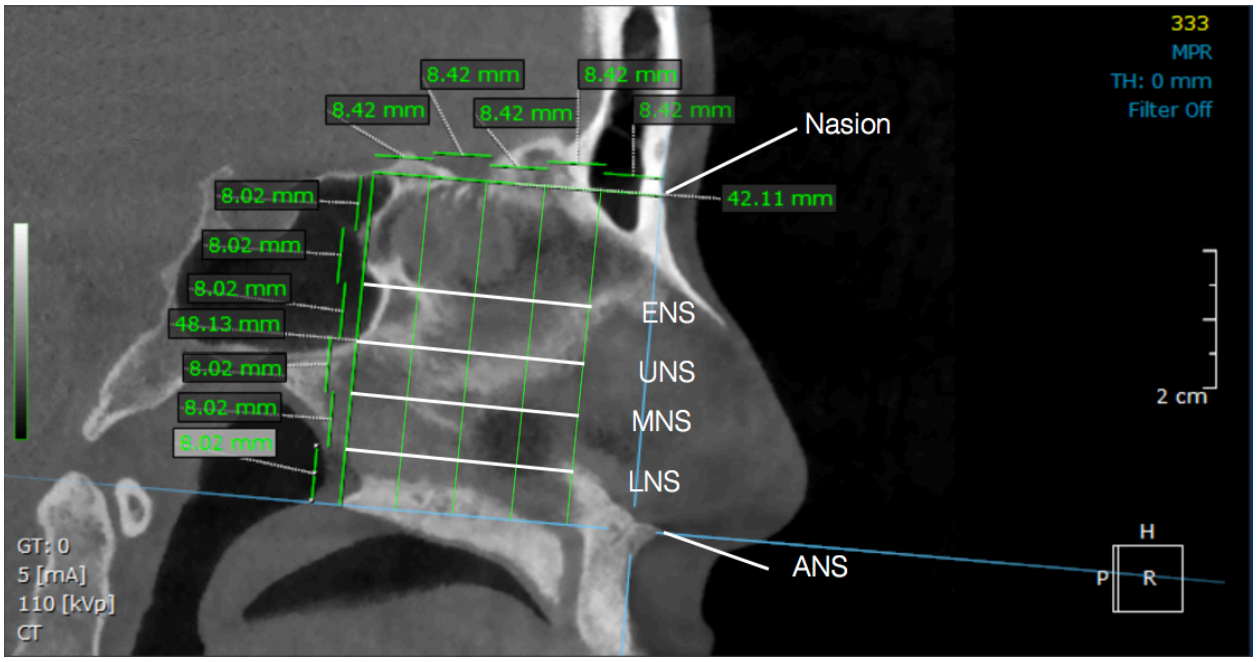

Figure 5: ENS, UNS, MNS and LNS; This Figure shows the cuts between Nasion and ANS and their description as ENS, UNS, MNS, LNS.

The average distance between the planes was 9.16 mm with a range from 8.15 mm to 9.95 mm.

The cross-points between the four horizontal and four vertical cuts resulted in a grid of 16 points on each side of the nasal cavity (Figure 6). On Figure 7 the measurement from those points from the left and right lateral walls of the nasal cavity to the MSP are displayed in the TNP. Overall a total of 32 measurements were done on each the pre-treatment and the post-treatment CBCT volume. A perfectly parallel expansion would demonstrate the same amount of change in the anterior and posterior region. A gradually decrease in the amount of expansion could be expected from the LNS to the ENS. All measurements were taken by the same examiner and an intra-rater evaluation

was carried out. A total of 25% of the sample was re-measured and the intra-class-correlation coefficient was calculated to be 96 %.

The results for each point were then averaged and an independent T-test was used to compare the increase in distance between the MSE and the Hyrax group. Statistical analysis showed that all 32 positions were highly significant with a p-value < 0.05.

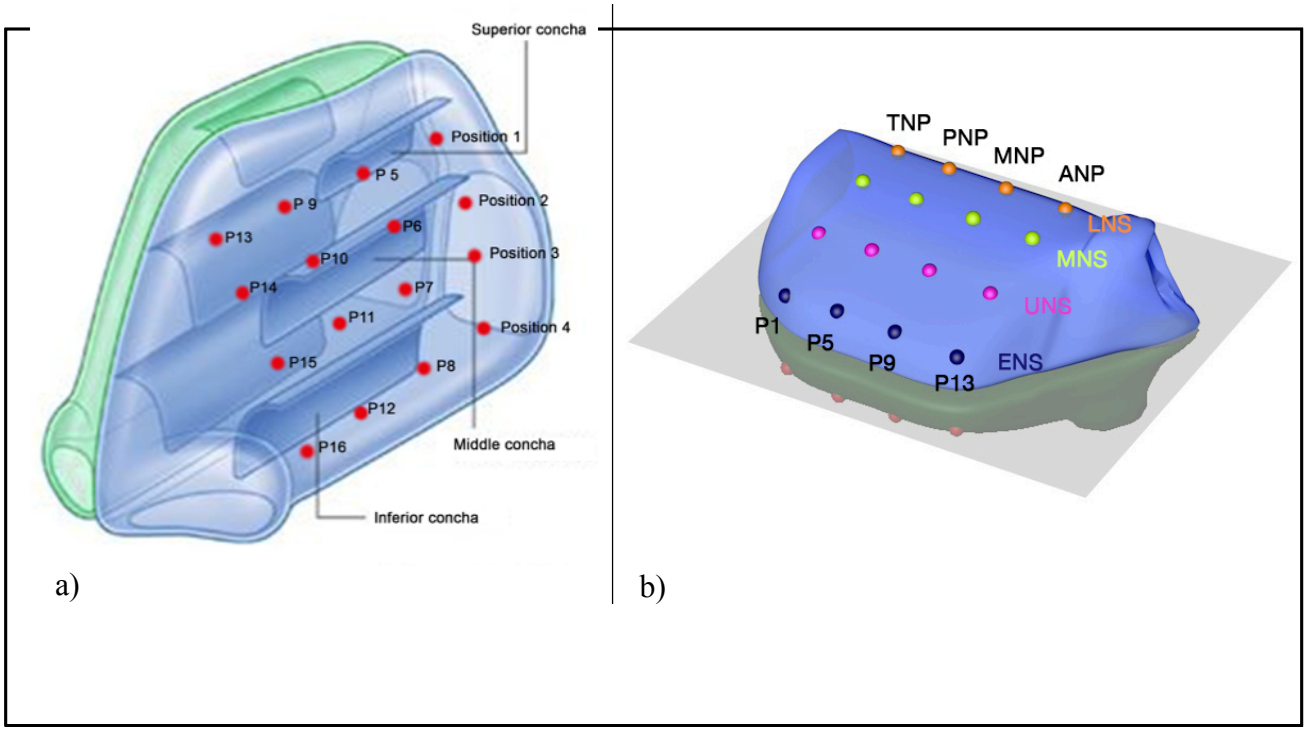

Figure 6: a) Measurement points; distribution of the measurement points on the lateral wall of the nasal cavity on the left side. The same points were also measured on the right side but are not displayed in the graphic. **b)** View of the nasal cavity from the top with the measurement points P1, P5, P9 and P13 labeled. This view will be used to display the results on 3D maps in the results section.

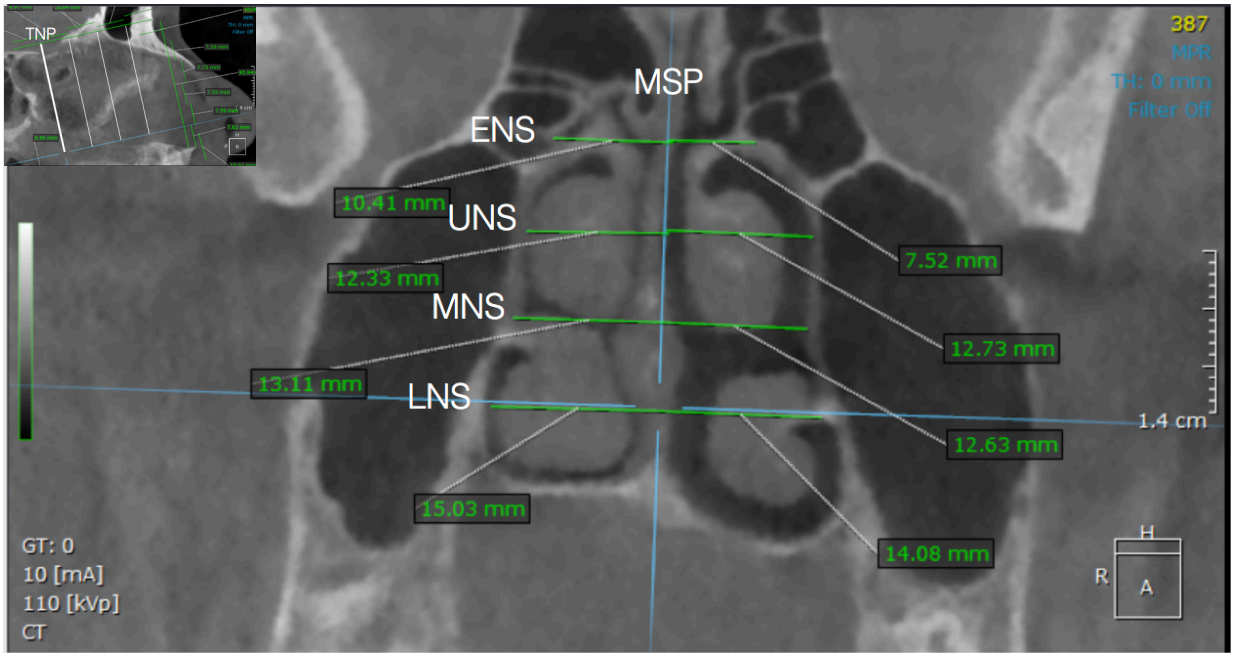

Figure 7: Cut through the TNP; displayed is a cut through the TNP and the measurements from the MSP to the corresponding points on the lateral walls of the nasal cavity on the ENS, UNS, MNS and LNS.

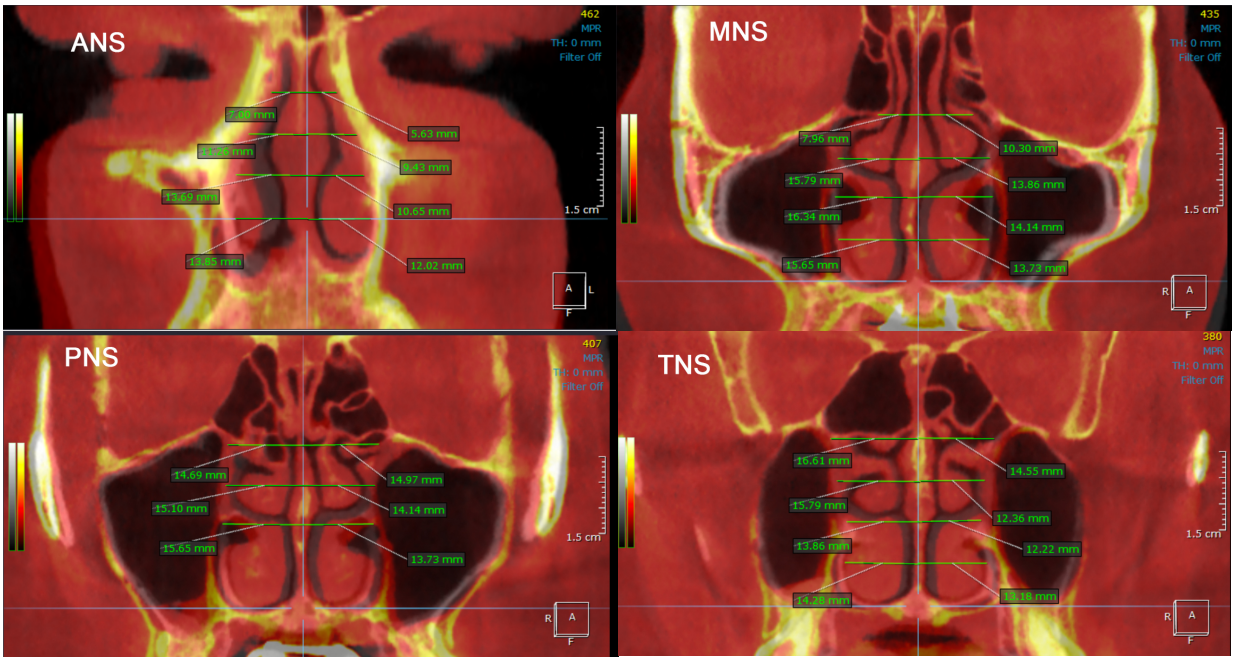

Figure 8: Coronal sections and measurements; these four pictures demonstrate the coronal sections in the different positions and the transverse measurements to the constructed points on the lateral nasal cavity walls.

Comparing the amount of change at each measurement point allowed then to establish the overall pattern of changes of the lateral walls of the nasal cavity. The results of changes for each patient are listed in Table 1 and Table 2.

Volumetric analysis of the air-filled spaces in the nasal cavity

In a second step the volumetric changes of the air-filled spaces in the nasal cavity were evaluated. These spaces are surrounded by mucosa and can vary greatly, depending on the mucosal swelling and de-swelling. The same CBCT scans used for the linear measurements were imported into ITK-SNAP Software (ITK) to execute the volumetric analysis by active contour measurement (38). Region of interest was set to be through Nasion, parallel to the maxillary plane in the horizontal and through anterior nasal spine and posterior nasal spine in the coronal plane. Laterally, the region of interest extended into the nasal sinus, enclosing the whole walls of the nasal cavity.

Segmentation was then carried out with Edge-attraction-settings and multiple seed points were distributed along the nasal cavity. The resulting volume included all air-filled spaces within the region of interest. In a next step, segmentations of the maxillary sinuses were removed manually by scrolling through the horizontal planes and using the eraser tool in each voxel-layer. This resulted in the final volume of the nasal cavity and the connected airspaces. Before and after treatment segmentation values were then entered in an excel spread sheet and the values analysed and compared.

Results

Measurement data

A total of 6 Hyrax patients and 16 MSE patient were found in the UCLA orthodontic clinic library that met the inclusion criteria. All the measurements were conducted as described above and the results are displayed in Table 1 and Table 2. Given are the pre-and post-expansion mean values for each point, as well as the standard deviations and the effective changes at each measurement point. The effective changes are also displayed in percentage in relation to the total transverse width in Table 3 and Table 4.

Position	Pre-mean	Pre-SD	Post-mean	Post-SD	Changes mean	Changes SD
1	9,97	7,20	10,08	7,24	0,11	0,23
2	22,83	3,58	23,28	4,03	0,45	0,53
3	24,29	4,11	25,47	4,10	1,19	0,51
4	27,55	4,04	29,19	4,83	1,64	1,07
5	17,07	8,74	17,57	9,09	0,51	0,71
6	26,17	5,09	27,06	5,02	0,89	0,64
7	26,32	2,73	27,51	2,76	1,19	1,07
8	28,62	1,34	30,63	1,59	2,01	1,45
9	16,09	5,35	16,23	5,34	0,14	0,16
10	25,43	3,17	26,33	3,10	0,90	0,58
11	27,80	2,39	28,95	2,10	1,15	0,60
12	30,91	1,78	32,83	2,02	1,93	1,13
13	13,17	5,14	13,36	5,01	0,19	0,22
14	20,87	2,86	21,67	3,08	0,79	0,69
15	23,19	3,61	25,32	4,69	2,13	1,30
16	24,06	3,21	26,28	4,39	2,22	2,13

Table 1: Hyrax measurements: This table displays the total transverse distance of the nasal cavity at each measurement point before and after, as well as the effective change in transverse width that occurred due to expansion therapy.

Position	Pre mean	Pre SD	Post mean	Post SD	Change mean	Change SD
1	14,10	6,19	15,48	7,25	1,38	2,00
2	24,91	3,35	26,80	3,45	1,88	1,16
3	24,73	2,75	27,57	2,61	2,84	1,38
4	29,51	2,28	32,76	2,30	3,25	1,32
5	13,19	6,95	14,01	6,81	0,82	0,72
6	26,02	4,25	27,54	3,89	1,52	1,19
7	25,48	3,17	27,78	2,91	2,31	1,30
8	31,27	2,02	34,86	2,31	3,59	1,48
9	14,53	3,24	15,72	3,48	1,19	0,60
10	25,22	2,99	26,45	3,38	1,23	1,19
11	30,41	3,59	33,10	3,66	2,69	1,05
12	31,51	2,19	35,94	2,50	4,43	1,39
13	12,99	2,77	14,90	3,01	1,91	1,12
14	21,44	4,67	23,89	4,79	2,45	1,48
15	22,72	2,90	26,01	3,88	3,28	1,69
16	24,66	2,37	29,13	2,95	4,47	1,43

Table 2: MSE measurements: This table displays the total transverse distance of the nasal cavity at each measurement point before and after, as well as the effective change in transverse width that occurred due to expansion therapy.

Position	Mean	SD	SEM
1	1,4%	2,6%	1,1%
2	1,8%	2,0%	0,8%
3	5,0%	2,4%	1,0%
4	5,8%	3,2%	1,3%
5	2,7%	3,3%	1,3%
6	3,6%,	3,3%	1,3%
7	4,6%	4,4%	1,8%
8	7,1%	5,2%	2,1%
9	0,9%	1,2%	0,5%
10	3,6%	2,6%	1,0%
11	4,2%	2,4%	1,0%
12	6,3%	3,7%	1,5%
13	2,2%	3,2%	1,3%
14	3,8%	3,2%	1,3%
15	8,8%	4,4%	1,8%
16	9,1%	8,3%	3,4%

Table 3: Hyrax percentage change; All the changes at each measurement point are displayed in percentages of the total transverse width at each point.

Position	Mean	SD	SE
1	9,5%	11,8%	3,0%
2	7,8%	5,4%	1,3%
3	11,8%	6,5%	1,6%
4	11,2%	4,9%	1,2%
5	7,8%	7,2%	1,8%
6	6,4%	7,0%	1,7%
7	9,4%	5,6%	1,4%
8	11,6%	5,0%	1,2%
9	8,3%	3,7%	0,9%
10	4,9%	4,6%	1,2%
11	9,1%	4,0%	1,0%
12	14,1%	4,6%	1,2%
13	15,4%	9,8%	2,5%
14	11,9%	7,4%	1,8%
15	14,4%	7,5%	1,9%
16	18,2%	6,0%	1,5%

Table 4: MSE percentage change; All the changes at each measurement point are displayed in percentages of the total transverse width at each point.

Hyrax Pre-treatment	Volume (mm^3)	SD	+/-
Left averaged volume	10,674.33	516.7904	186.0376
Right averaged volume	11,037.00	509.0794	176.6814
Total averaged volume	21,711.33		

Table 5: Nasal cavity air volume in the Hyrax group pre-treatment

Hyrax Post-treatment	Volume (mm^3)	SD	+/-
Left averaged volume	12,803.83	512.014	189.4956
Right averaged volume	13,960.33	515.9686	186.8959
Total averaged volume	26,764.17		

Table 6: Nasal cavity air volume in the Hyrax group post-treatment

MSE Post-treatment	Volume (mm^3)	SD	+/-
Left averaged volume	10,481.00	463.4996	175.7245
Right averaged volume	9938.06	449.1738	172.2818
Total averaged volume	20,419.06		

Table 7: Nasal cavity air volume in the MSE group pre-treatment

MSE Post-treatment	Volume (mm^3)	SD	+/-
Left averaged volume	13,695.00	477.159	200.5681
Right averaged volume	12,730.69	470.5434	191.203
Total averaged volume	26,425.69		

Table 8: Nasal cavity air volume in the MSE group post-treatment

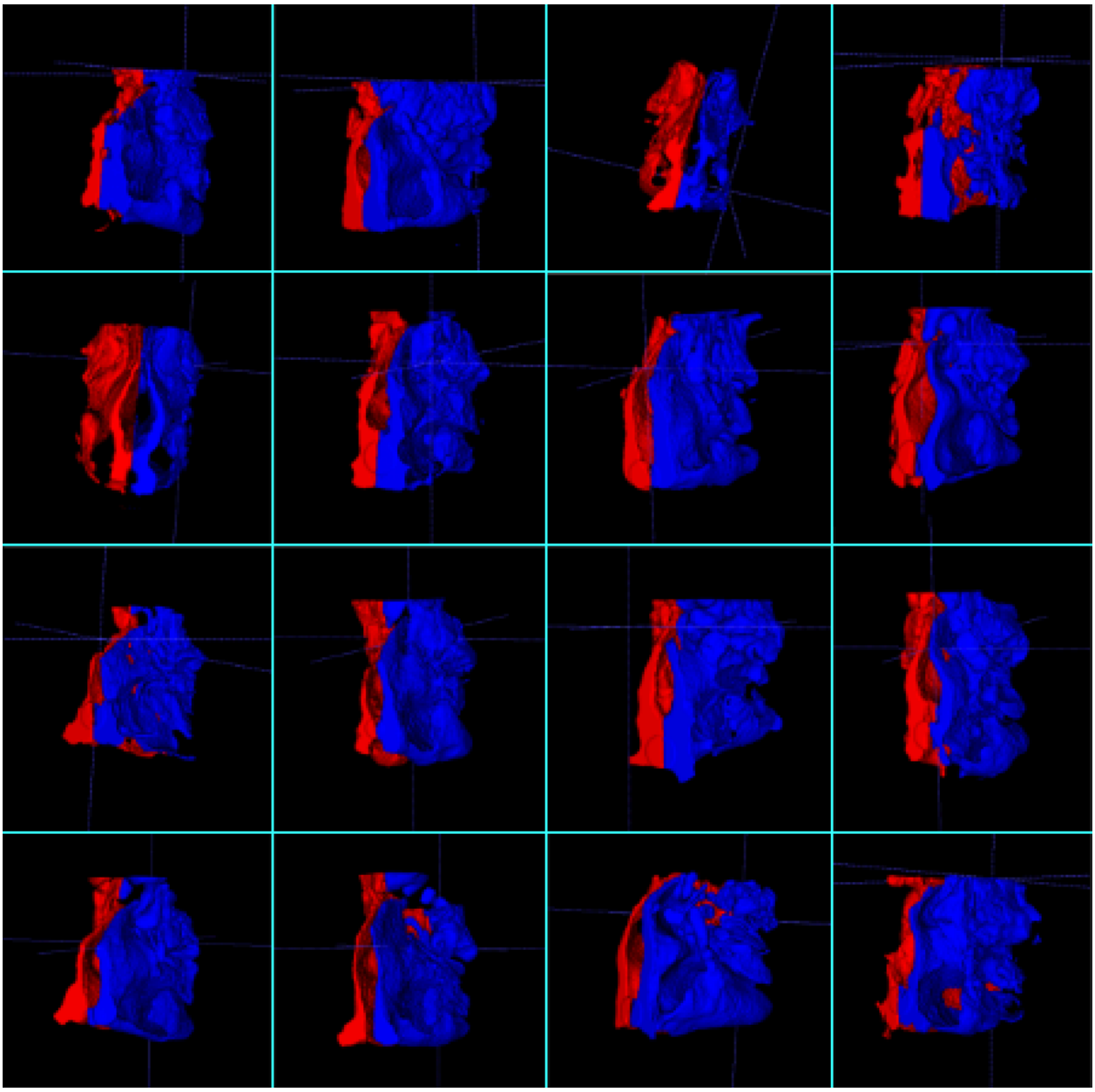

Figure 9: Collage of the post-expansion volume rendering of the air spaces in the nasal cavity of the MSE group.

Table 5 to Table 8 show the pre- and post-treatment volumetric measurements of the nasal cavity in the Hyrax and the MSE group. The mean initial total volume is 21,711.33 mm^3 in the Hyrax group and 20,419.06 mm^3 in the MSE group. Post treatment means are 26,764.17 mm^3 in the Hyrax group and 26,425.69 mm^3 in the MSE group. This

results in an overall volume increase in the Hyrax group of 5052.83 mm^3 or 23.27% and 6006.68 mm^3 or 22.73% in the MSE group.

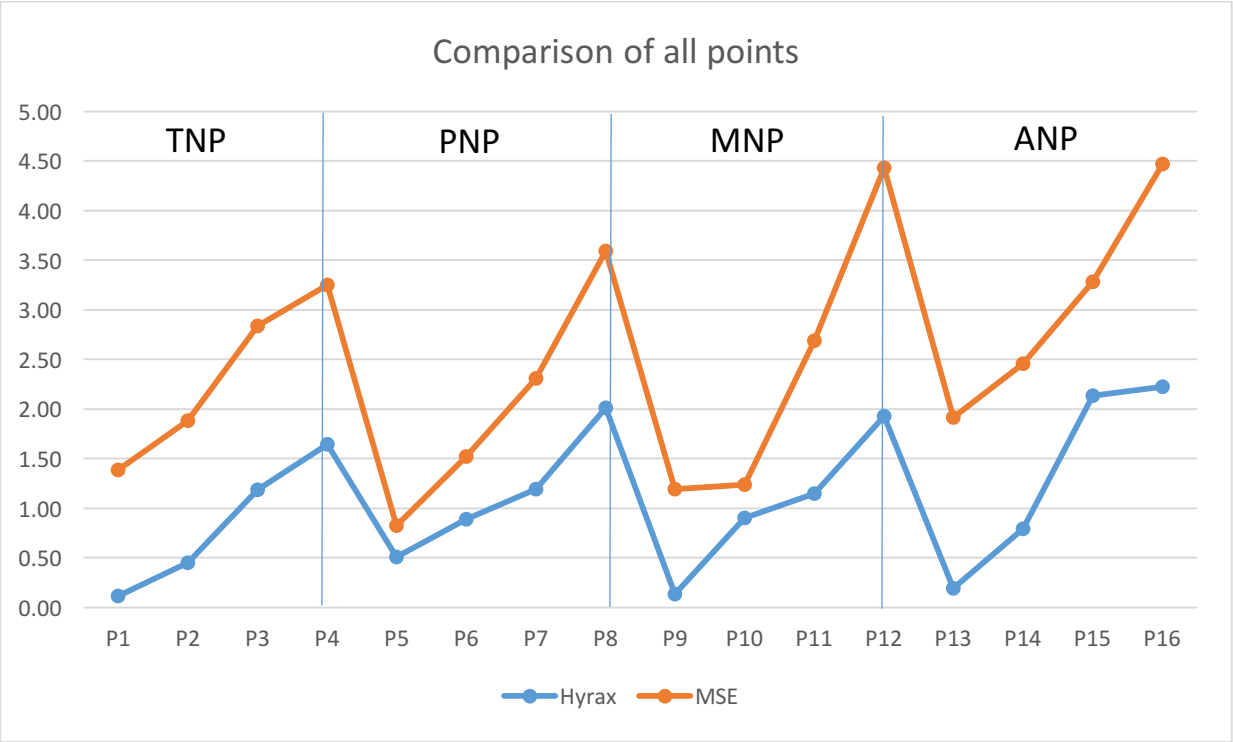

Figure 10: Comparison of all points.

Figure 10 displays the combined change of left and right at each measurement point. P1, P5, P9 and P13 are representing the amount of expansion at the ENS, while P4, P8, P12 and P16 represent the expansion at the LNS.

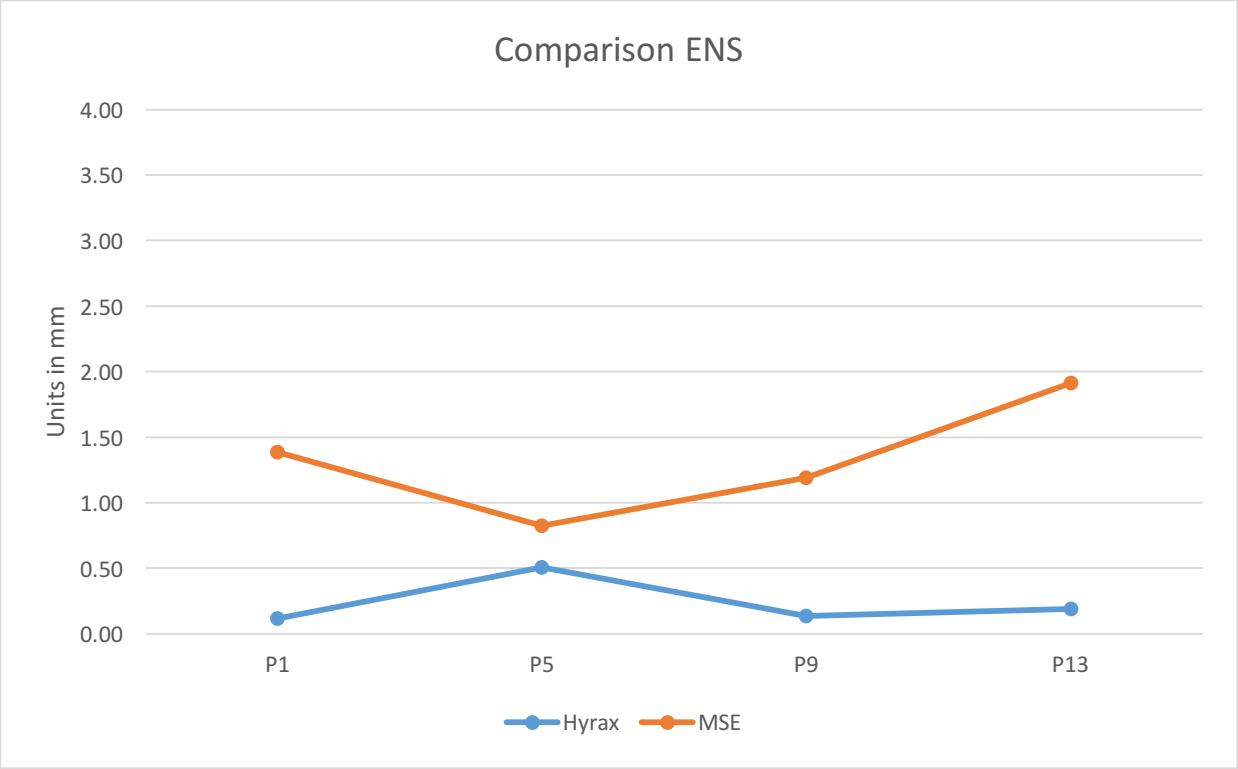

Figure 11: Comparison ENS

Figure 11 displays the changes in the ENS. While the Hyrax expansion had almost no effect at this level of the nasal cavity, the MSE appliance was able to achieve significant expansion in this area.

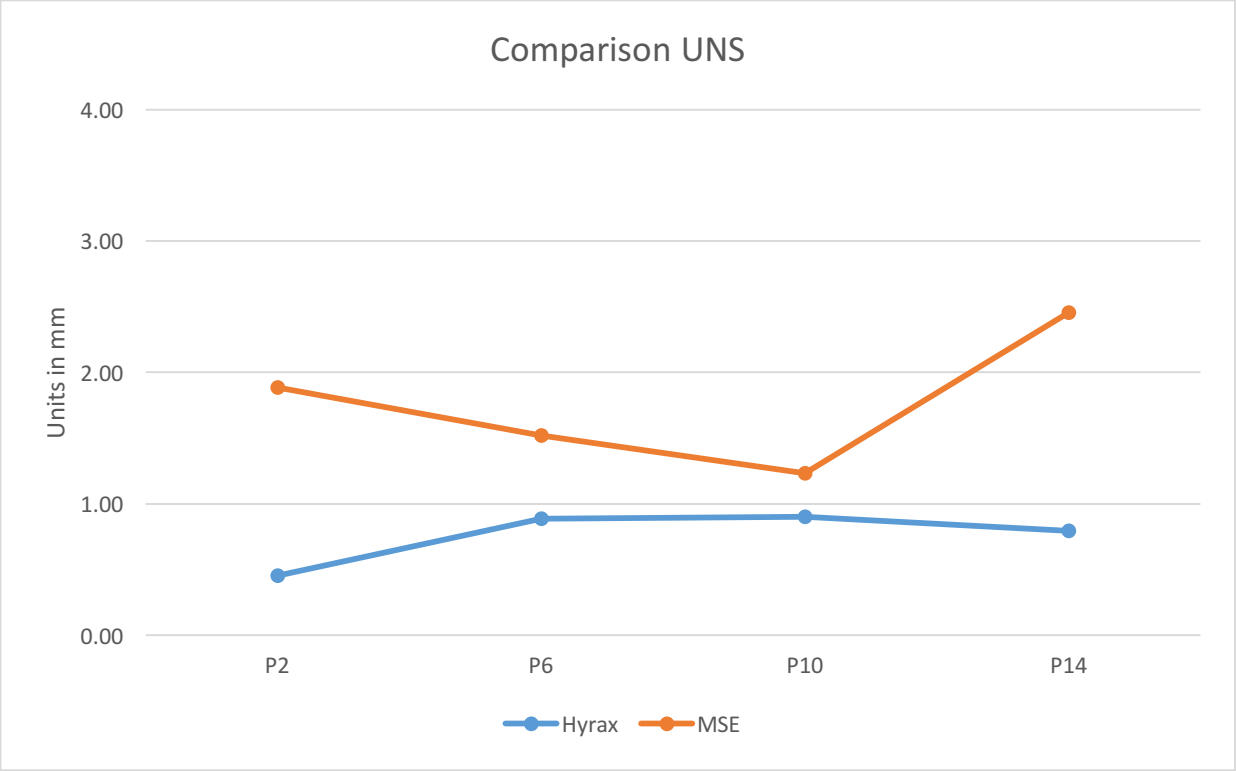

Figure 12: Comparison UNS

Figure 12 shows that the Hyrax expansion effect at the UNS was 0.45 mm in the posterior, but increased in the anterior to 0.79 mm and led to an almost parallel widening of the nasal cavity. The MSE demonstrated an overall larger expansion but had less effect in the P10 region.

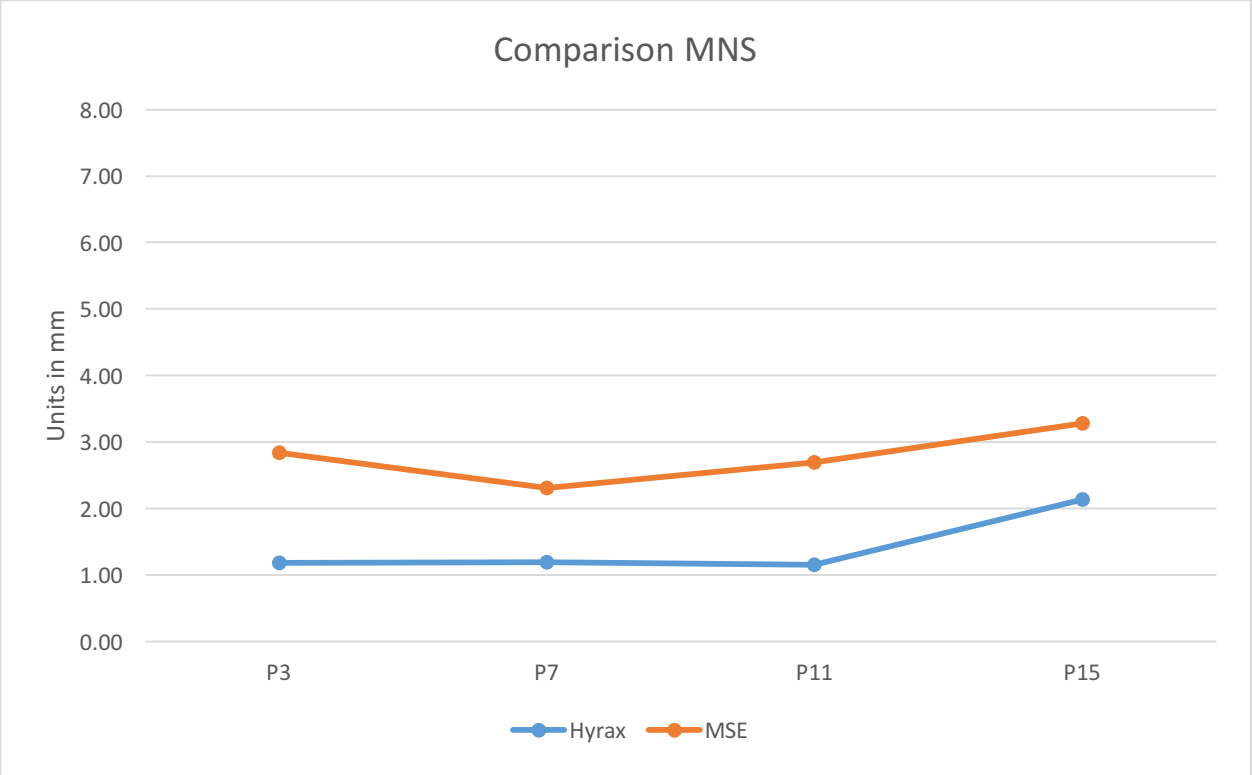

Figure 13: Comparison MNS

Figure 13 shows that the Hyrax appliance resulted in an average expansion of 1.19 mm in the posterior P3, and 2.13 mm at the anterior P15.

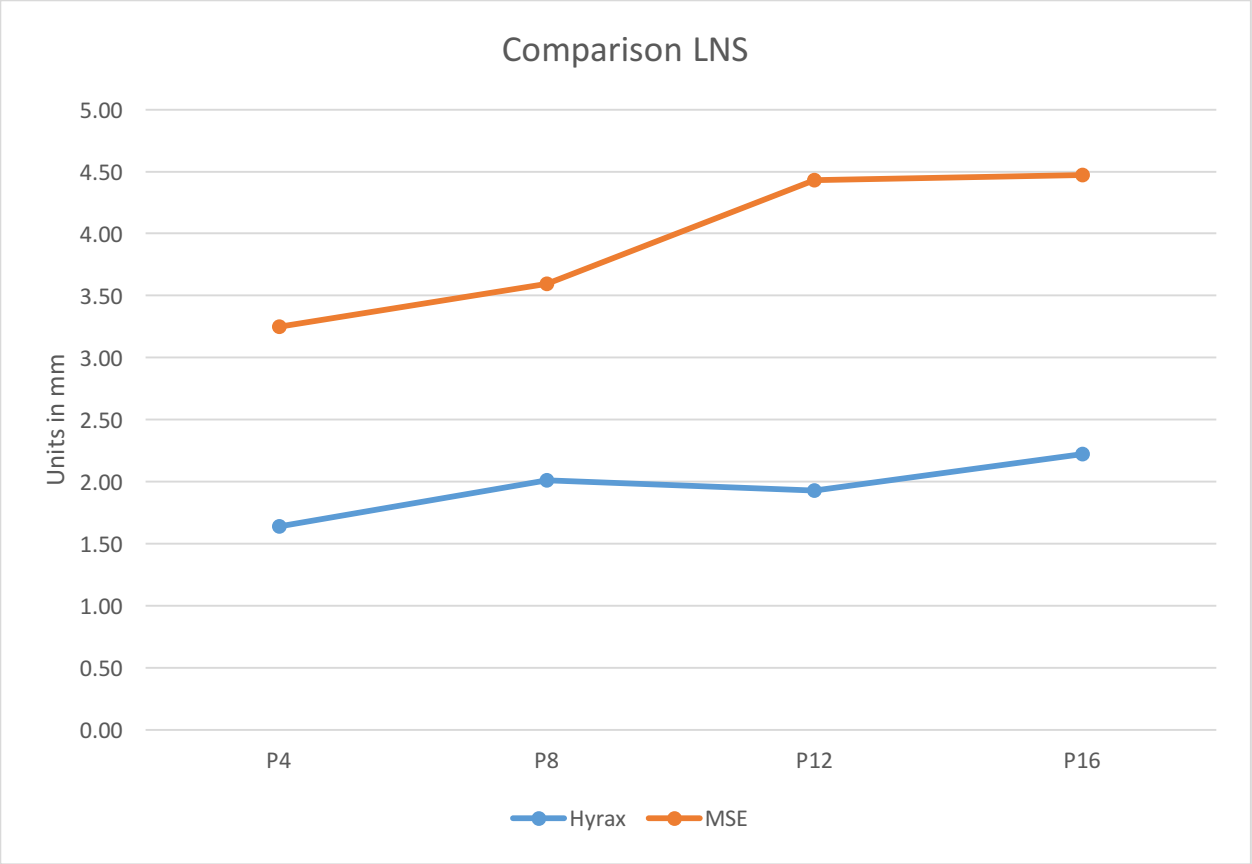

Figure 14: Comparison LNS

The Hyrax expansion in the LNS displays an overall slight increase from posterior to anterior from 1.64 mm to 2.22 mm, with a difference of 0.58 mm (Figure 14). In the MSE group the increase ranged from 3.25 mm at P4 to 4.47 mm at P16, with a antero-posterior difference of 1.22 mm. Most of this change occurred between P8 and P12, with a difference of 0.83 mm.

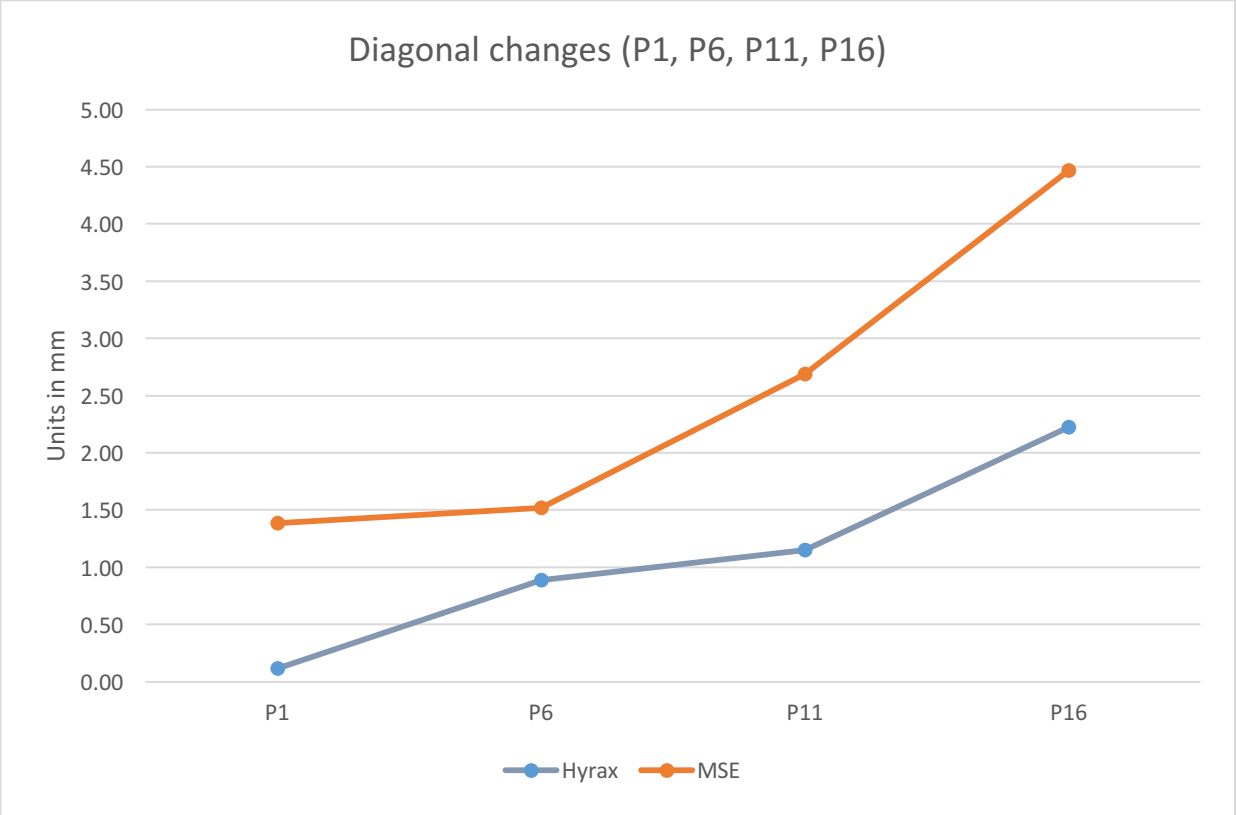

Figure 15: Diagonal changes (P1, P6, P11, P16)

In Figure 15 the points were connected from the posterior-superior to the anterior-inferior. The expansion amount increased from 0.11 mm to 2.22 mm in the hyrax and from 1.38 mm to 4.47 mm in the MSE. While the increase in the Hyrax group appears to be almost linear, the increase in the MSE group is little between P1 and P6, but then almost doubles at P11 and P16.

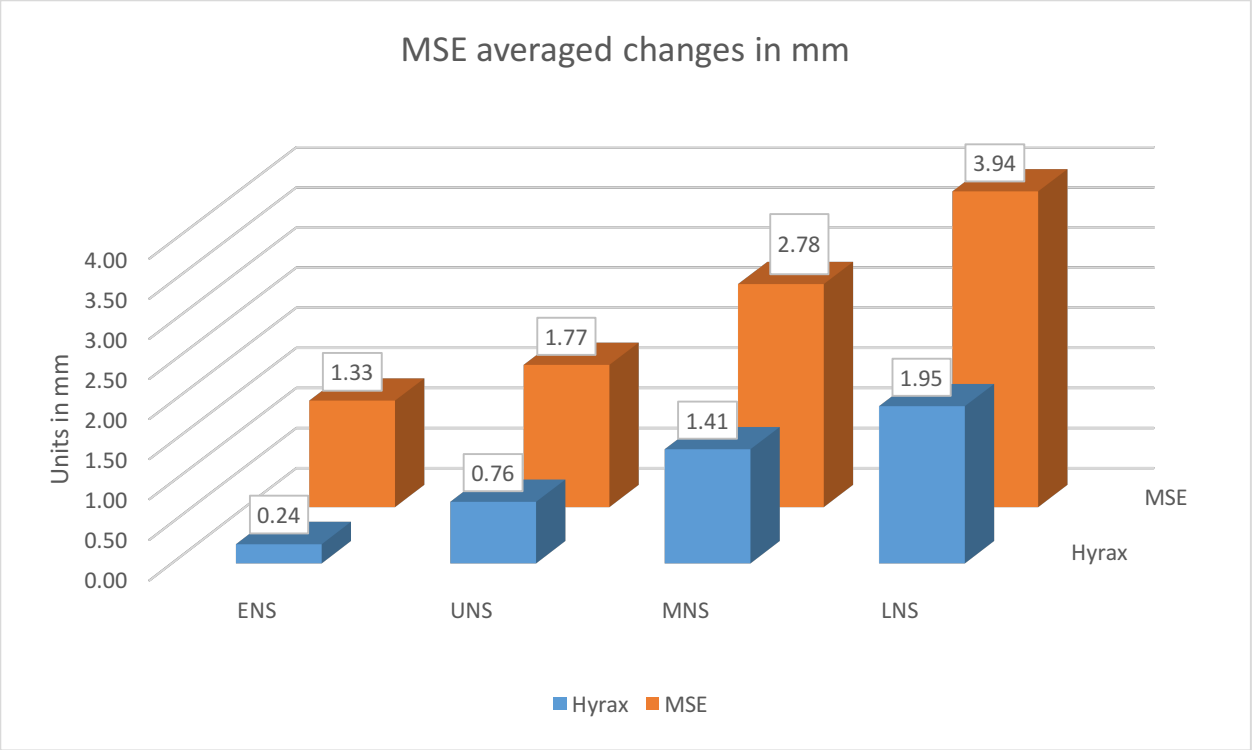

Figure 16: MSE averaged changes in millimeter

Figure 16 shows the mean changes at the different horizontal sections, indicating a gradual increase in expansion effect from 0.24 mm to 1.95 mm in the Hyrax and from 1.33 mm to 3.94 mm in the MSE group.

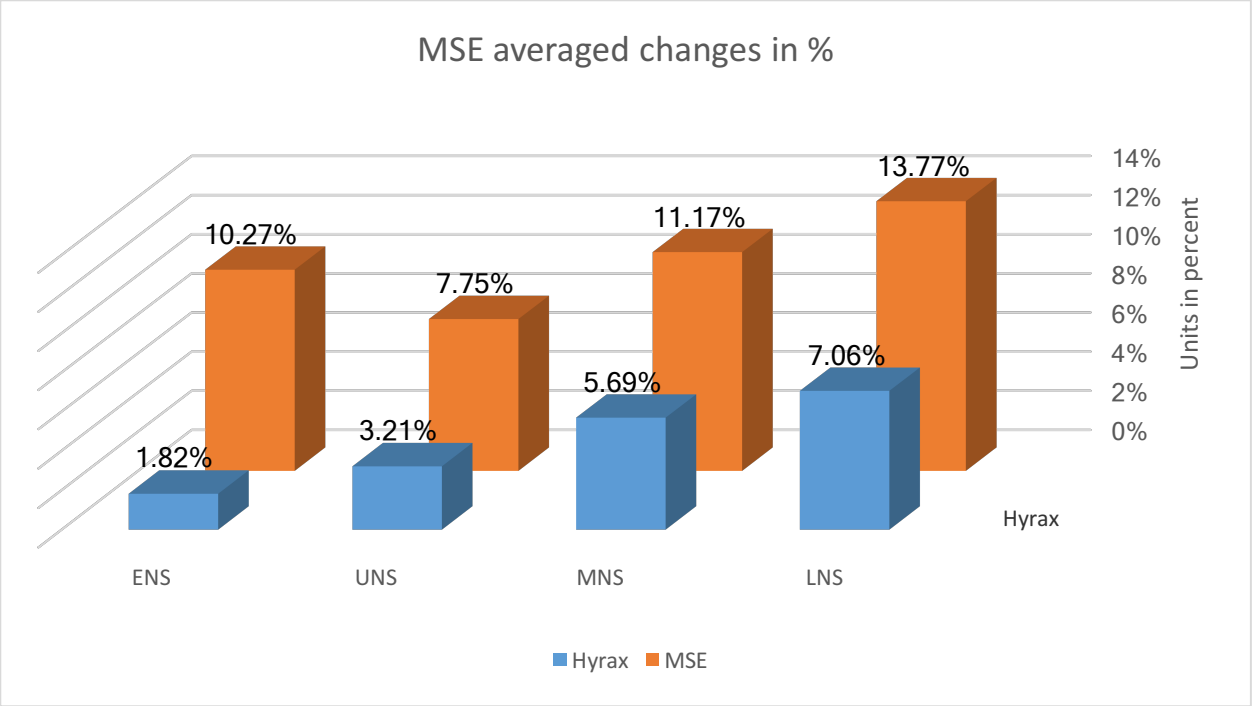

Figure 17: MSE averaged changes in percent

In Figure 17 the amount of expansion change is displayed in percentage and one can see the increase of expansion effect from the ENS from 1.82% to 7.06% in the LNS in the Hyrax group. Meanwhile the expansion effect in the MSE group stayed quite consistent between 7.75% in the UNS and13.77% in the LNS.

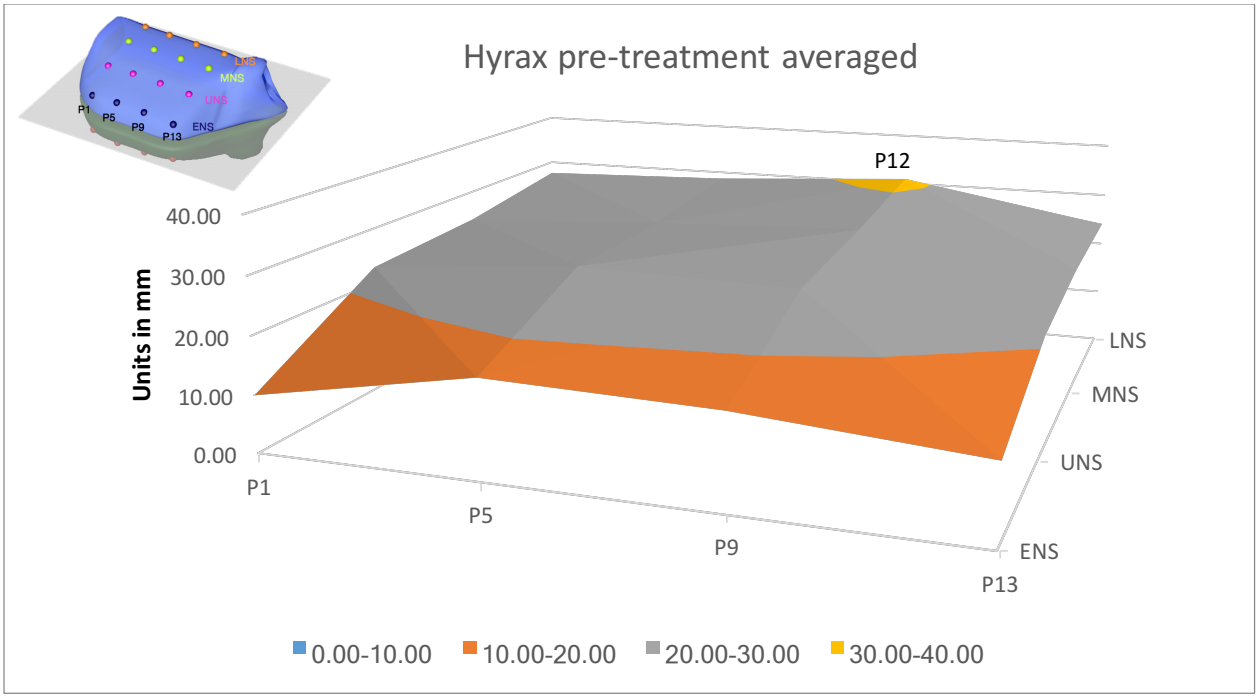

Figure 18: Hyrax pre-treatment averaged

The map in Figure 18 represents the morphology of the nasal cavity by displaying the mean total distances of each corresponding point pre-treatment in the Hyrax group. One can see, that the width of the nasal cavity is greater in the lower sections, with the largest distance at point P12 (in yellow). The orange area represents the total transverse width of the nasal cavity of 10-20 mm, which corresponds with the ENS and partially UNS.

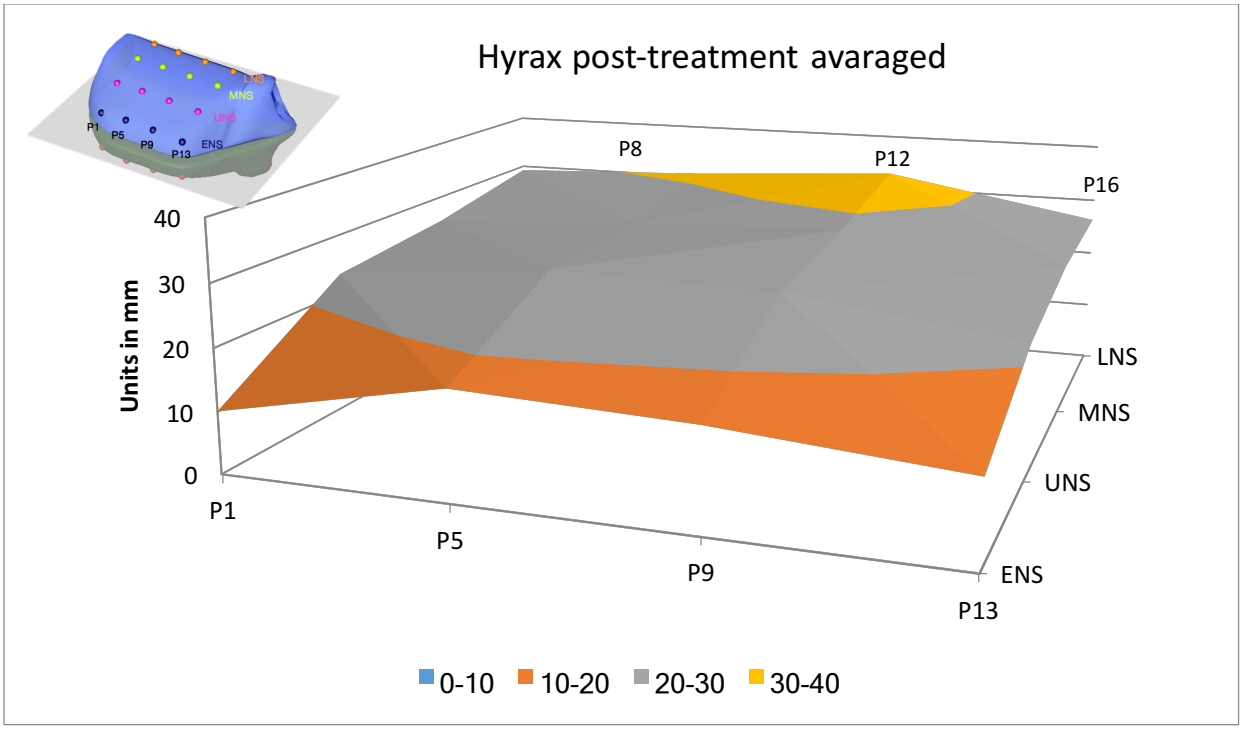

Figure 19: Hyrax post-treatment averaged

In Figure 19 the map represents the morphology of the nasal cavity by displaying the mean total distances of each corresponding point post-treatment in the Hyrax group. One can see that the yellow area stretches from P8 to P12 and half way to P16. The orange area, represents the narrowest part of the nasal cavity, which is in the ENS and partially UNS.

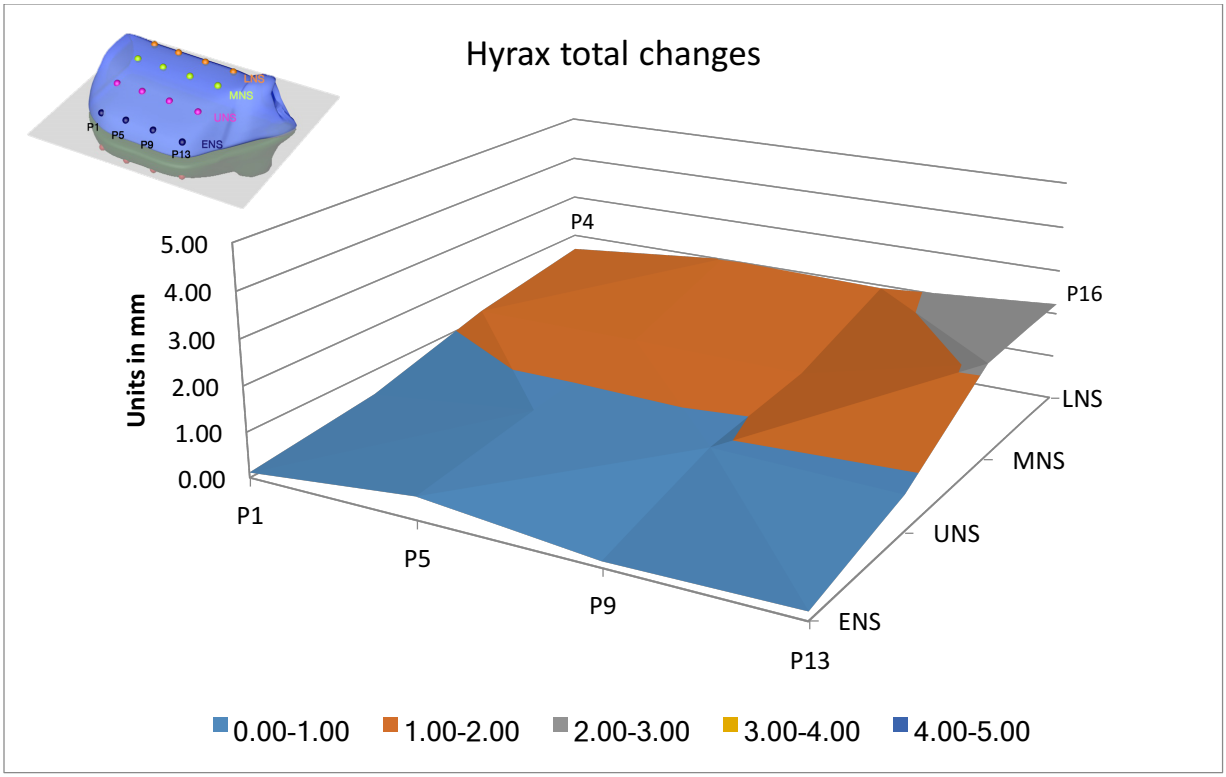

Figure 20: Hyrax total changes

When the total expansion-changes in the Hyrax group are displayed on a 3D-map in Figure 20, one can see that the largest effect is in the LNS, with a value of P16 of 2.22 mm and P4 with 1.64 mm. The changes in the ENS are minimal and range from P1 0.11 mm to 0.51 mm at P5.

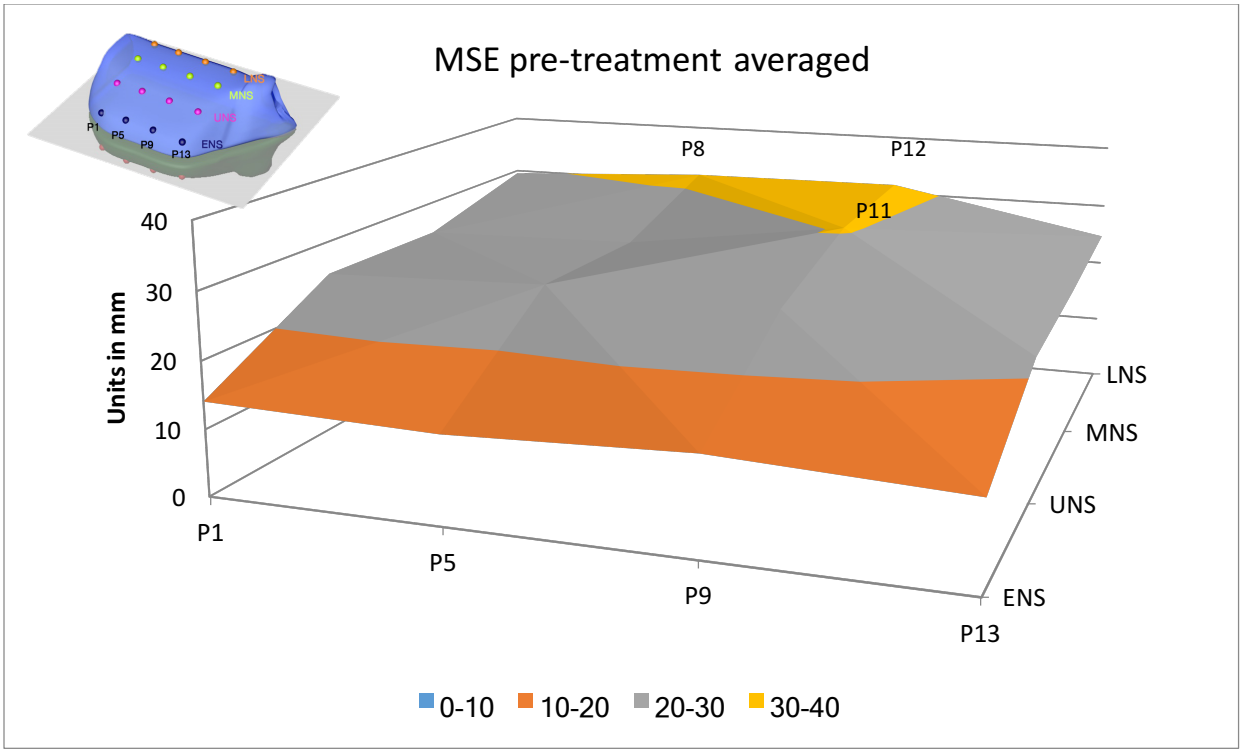

Figure 21: MSE pre-treatment means

The graphic in Figure 21 presents the pre-treatment transverse distances of the nasal cavity at each measurement point. The largest distances are at P11, P12 and P8 at the LNS. The smallest distances are at P1, P5, P9 and P13 at the LNS.

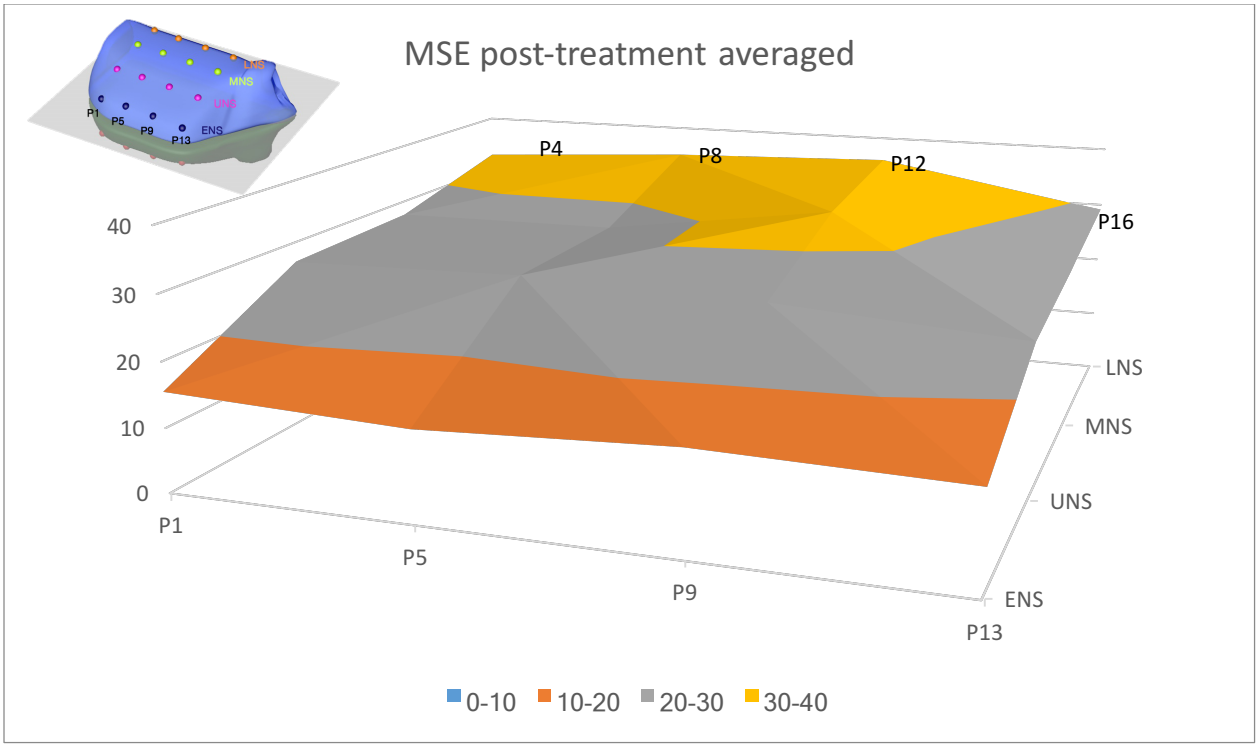

Figure 22: MSE post-treatment means

After the expansion, the transverse distances at the measurement points increased, visually presented by an enlarged yellow area in the LNS at P4, P8, P12 and P16 in Figure 22. The increase in the ENS is only minimal, but still noticeable.

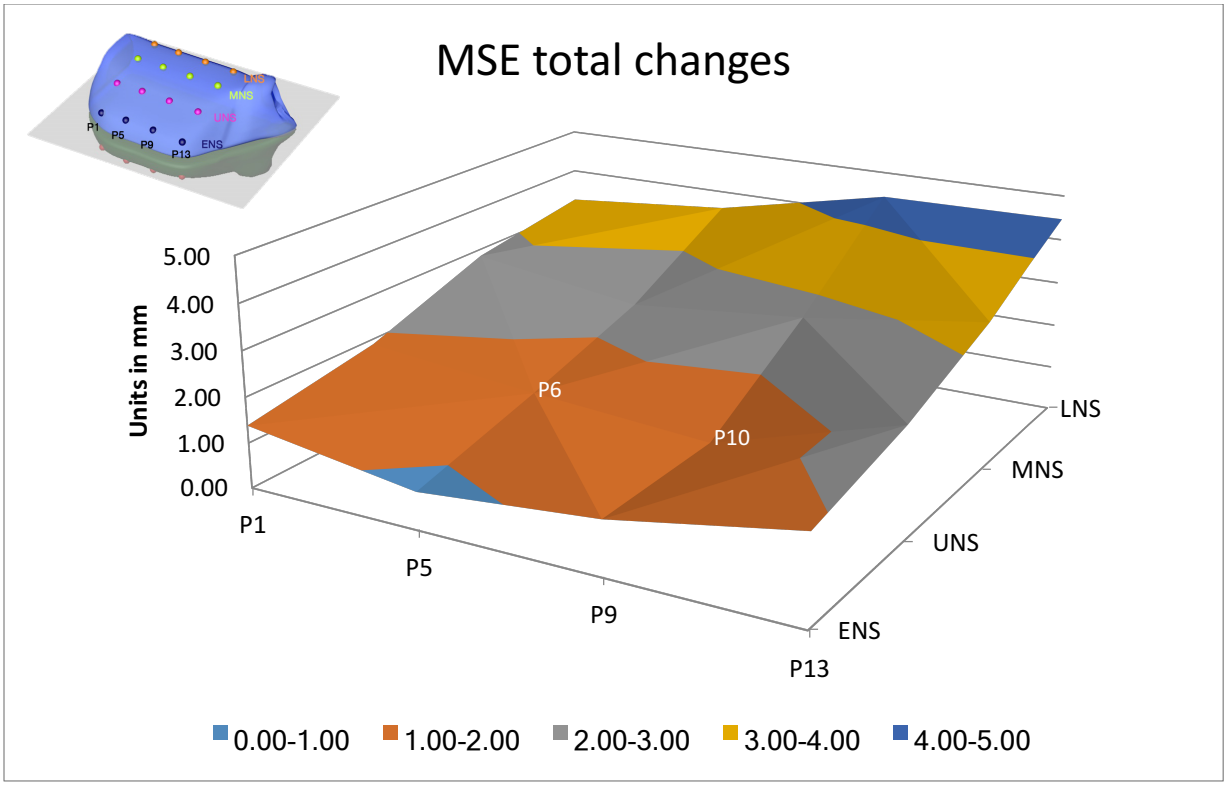

Figure 23: MSE total changes

For Figure 23, the left and right pre-expansion distances were subtracted from the post-treatment distances. This demonstrates the effective expansion amount at each measurement point and it is apparent that most of the expansion happens in the LNS and MNS, with the largest effect on P16 in LNS. There is a reduced effect on P5, P6 and P10.

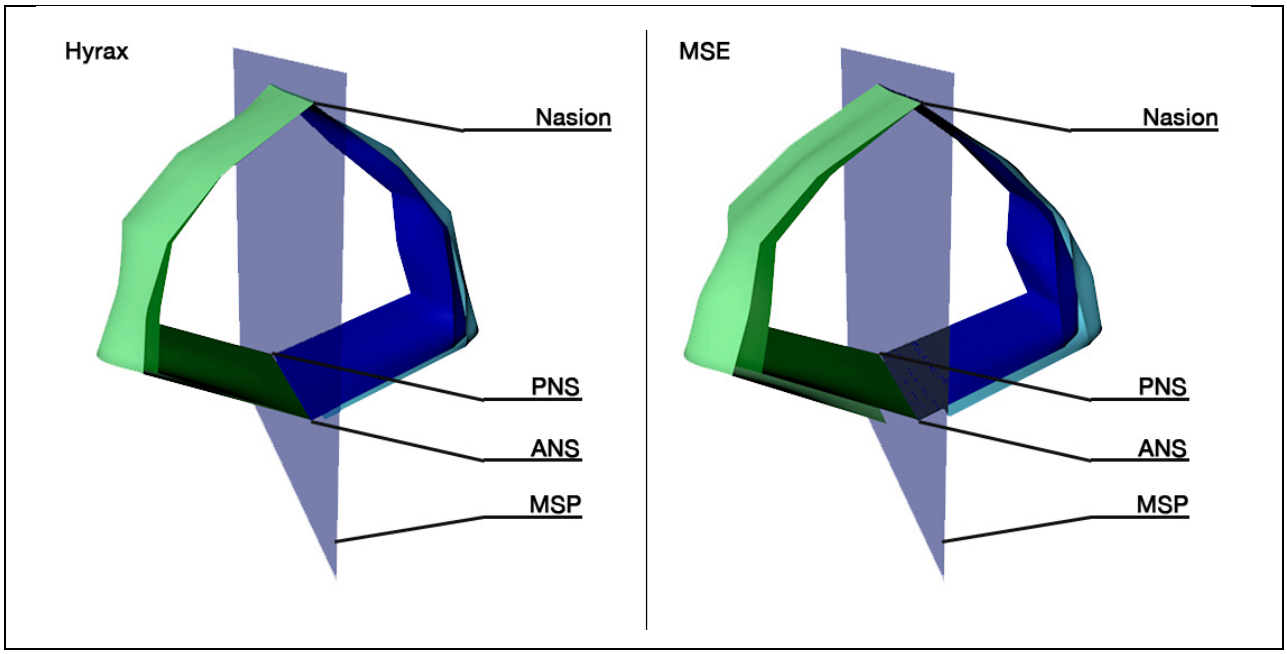

Figure 24: 3D-display of the expansion effects on the nasal cavity. Left side is the Hyrax group and right side is the MSE group.

In Figure 24 the expansion effects of the Hyrax and MSE groups are displayed and compared. Pre-expansion nasal cavity is displayed in dark blue and dark green, while post-expansion is in light blue and light green. One can see that expansion with Hyrax appliance affects the lower part of the nasal cavity with small separation of the right and left halves. Expansion with MSE has a far larger effect on the lateral walls of the nasal cavity and a bigger separation of the right and left halves occurs.

Discussion

Several studies on rapid palatal expansion effects on the airway were conducted during the last decades. Many of these studies investigated the changes in nasal cavity by superimposing 2-dimensional x-rays, being limited by lack of details and structural superimpositions which makes it difficult to evaluate precise anatomic boarders and landmarks. Quality and resolution of current cone-beam CT imaging techniques is reported in the literature to be of sufficient accuracy to measure the nasal cavity(39-41). The method of choice to compare treatment changes is to superimpose the pre- and post-treatment scans on stable landmarks, such as the cranial base, as described by Bjork(42) and Doppel(43). Development of novel computer software algorithms allow nowadays to accurately superimpose 3D-CBCT images on these stable structures, with a minimal margin of error(44). The superimposition method used in this study is a voxel-based rigid registration, fully automated and observer independent. This method compares the grey-scale of each voxel in the cranial base and computes the best fit, reducing the margins of error and resulting in a consistent and reliable comparison of the CBCT data(45-47). The OnDemand3D software by Cybermed Inc. then allows to graphically overlay the different time points and manually select points of interest, establish reference planes, measure distances, or if needed, calculate angles.

The method used in this study to establish the reference planes was described by Cantarella(29) and allows to analyze the movements of skeletal changes induced by rapid palatal expansion. Especially important is the midsagittal plane, which is established by connecting the most reliable anatomic landmarks that can be found in this cut – namely the anterior nasal spine, posterior nasal spine and nasion. Remaining

planes were then based on the first one and positioned perpendicular to it. All landmarks were tested for inter-rater reliability with Intraclass Correlation Coefficient (ICC) and resulted in an ICC of 93.5% for the linear measurements, showing a high reliability. Combination of the grey-scale based superimposition technique and utilization of the reference planes allows to establish an individualized reference grid to accurately represent the expansion effects on the lateral walls of the nasal cavity and demonstrate the overall expansion pattern.

In 2012, Ribeiro tried to overcome the limitations of 2-dimensional x-rays by using cone-beam CT images of 15 patients in mixed dentition with an average age of 7.5 years. The images were manually aligned and the nasal cavity was divided into 3 sections, each 15mm apart from each other. Only the width changes in the lower nasal section were measured, but demonstrated a significant increase after the expansion(30). One significant limitation of this study was that a pre-set distance between the sections of 15 mm does not allow to adjust the measurements relative to the actual length of the patient's nasal cavity. In the present study, it is attempted to overcome this limitation by dividing the distance between ANS and PNS into 4 equal sections, allowing for a relative adjustment to each patient's individual length between ANS and PNS. Besides this, the method further resulted in each section being better comparable to the full sample and enabling transverse measurements in these sections to be more comparable. A vertical grid was added following the same method, only dividing the distance from Nasion to the palatal plane, a line connecting anterior nasal spine and posterior nasal spine. In this way, the grid is adjusted to each individual patient and

reference points more likely represent similar areas when patients are compared to each other.

When the maxilla is subjected to expansion in the Hyrax group, the midpalatal suture separates in a v-shaped pattern with greatest separation in the anterior and least separation in the posterior (4). Lione described that expansion at PNS was 65% of ANS and the transverse width of the lower nasal cavity increased in a similar fashion(10). Wertz stated, that this is due to the interlocking pyramidal processes of the palatine bone with the immovable medial and lateral pterygoid plates of the sphenoid bone when expansion is attempted with a tooth-borne expander(48). However, this changes throughout the nasal cavity and Ribeiro reported, that the expansion pattern of the lower nasal cavity was greatest in the middle section, followed by the anterior and the posterior(30). Interestingly a different pattern of expansion was seen in this study. Looking at the individual sections, one can see that almost no expansion happened in the most upper ENS. As a tooth-borne appliance was used and this section is surrounded by the walls of the orbits, the orbital rims and in proximity to the cranial base, no changes were expected. At the other sections, namely the UNS, MNS and LNS the largest amount of expansion occurred close to the anterior nasal spine at P16. The absolute amount of expansion reduced gradually further up and backward (P15, P12, P11). This can be clearly seen in Figure 10.

During the expansion procedure with MSE, peri-maxillary sutures disarticulate allowing a larger rotational movement of the maxillary halves and an almost parallel split of the midpalatal suture (29). Again, even though the pattern of expansion at the palatal level

is far more parallel compared to the Hyrax group, the expansion of the lateral walls of the nasal cavity does not follow this pattern.

Figure 11 displays the ENS and it can be seen, that there is a varying but significant amount of increase in transverse width with MSE expansion. It is less in the posterior and increases in the anterior. Disarticulation of the nasomaxillary sutures as a result of this type of expansion was reported before by MacGinnis (49), who stated that the maxillary halves rotate laterally and downward around a center of rotation in the midline between the orbits(29), close to the cranial base. P1 is the measurement point closest to the cranial base and thus the center of rotation and should show the least changes. While this is true in the Hyrax group, it is not for the MSE group. Here P5 is the point with the least amount of change. A possible explanation could be that the actual center of rotation for the maxillary halves during the expansion is not close to the cranial base, but further lateral at the frontozygomatic sutures. The largest movement occured as expected furthest away from the center of rotation at P16, closest to the nasomaxillary suture.

At the next section, UNS, in Figure 12, there is an almost parallel, minimal effect from the Hyrax appliance, while expansion with the MSE was overall 230% larger, with the least amount of expansion at P10 (1.23 mm) and increased effects posterior at P2 (1.88 mm) and anterior at P14 (2.45 mm). This can be explained by the different densities of the bones in the different planes, with only thin lateral walls of the nasal cavity in the posterior and the thicker and stronger orbital rims in the P10 area. Different amount of expansion, although only 1.22 mm (P13 minus P10), means that the lateral walls bend under the force load and did not follow a linear pattern as would have been expected in

a uniform plane. In 2007, Palaisa analyzed the cross-sectional areas of the nasal cavity in three cuts and observed that the increase in transversal areas of the anterior, middle, and posterior nasal cavity was larger than in the middle (8.77 cm^2) and posterior areas (9.13 cm^2) in relation to the anterior area (7.31 cm^2) of the nasal cavity. This confirmed that expansion of the nasal cavity with a Hyrax appliance does not necessary follow the standard triangular opening of the midpalatal suture (31).

The next section is the MNS (Figure 13) where the same pattern as in the UNS repeats in a decreased manner. The effective, averaged amount of Hyrax expansion almost doubled compared to the UNS and the expansion pattern is overall more parallel in both groups. The expansion effect of MSE is with a mean of 2.78 mm, 196% larger than the Hyrax group. Still the largest changes happened in the anterior area at P15.

The LNS (Figure 14) is closest to the palate and the expansion device and therefore displays the largest amount of transverse change compared to the other sections. Averaged Hyrax expansion was 1.95 mm, while MSE achieved 3.94 mm, again 202% the amount. Only a mild gradual increase from posterior P4 to anterior P16 was seen in the Hyrax group, while the MSE group showed a significant transverse increase happened between posterior P4 and the more anterior P12, and no change P12 and P16.

Overall, the MSE group had double the amount of expansion compared to the Hyrax group. Generally, the expansion pattern was similar, with little effects in the posterior, superior regions close to the cranial base and near the higher density bones at the orbital rims. The walls of the nasal cavity do not expand in a linear pattern, but rather

bend under the pressure and distort to follow the rotational movements of the maxillary halves. If one compares the expansion pattern in a diagonal fashion (Figure 15) from posterior superior to anterior inferior, P1, P6, P11, P16, the Hyrax appliance displays a linear increase in its expansion effects from 0.11 mm to 2.22 mm, while the MSE appliance demonstrates an almost exponential effect from 1.38 mm to 4.47 mm.

Besides, the fact that the absolute amount of expansion decreases the further away from the expander and the closer to the center of rotation one gets, it is interesting to look at the percentile changes of the transverse width before and after expansion in Figure 17. In the Hyrax group, the largest increase is 7.06% in the LNS, with a gradual decreased effect to 1.82% in the ENS. The MSE group displays a far more consistent increase of transverse size, with a maximum of 13.77 % in the LNS and a minimum of 7.75% in the UNS and 10.27% in the ENS. It becomes obvious that Hyrax expansion mostly affects the lower part of the nasal cavity and less so the upper regions. Due to the mini-screw supported anchorage and better force delivery system of the MSE, the center of rotation of the maxillary halves is more coronal (29). This allows for larger effects on the lateral walls of the nasal cavity. Changes of 10.27% in the ENS might be partially due to the overall small amount of transverse effects in this area, and small measurement errors might get magnified in this type of presentation of the data.

When one compares the total changes between the Hyrax and the MSE groups in Figure 20 and Figure 23, the effects of the Hyrax expansion are overall less: the pattern describes the typical V-shaped expansion with little effects in the posterior and the most effect in the anterior. Effects decrease rapidly as one moves from the palate towards the cranial base and are negligible in the ENS. MSE total changes are different, not only are

they in average two times greater than in the Hyrax group, but they also are more continuous and extend all the way to the ENS, showing a clear increase the width close to Nasion and dorsal of it. Even points close to the cranial base demonstrate measureable changes, though probably clinically insignificant.

Increased changes of the nasal cavity in the MSE group can be attributed to the usage of four miniscrews with bicortical engagement in the palate. As described by Lee (50) in a finite element analysis, bicortical engagement of the screws allows to deliver higher forces to the bone while simultaneously reducing stress induced, pathologic fractures and bone resorption. This further allows to reduce the stress level at the bone-implant interface, leading to reduced chances of screw deformation or fracture. It was also found that the transverse displacement of the maxillary halves is significantly increased at each activation turn in the model with bicortical engaged miniscrews (50). Based on this FEA model and the results from this study, it becomes clear why MSE can affect the nasal cavity in such greater magnitude and achieve expansion not, only in the lower section like a tooth-borne expander, but also affects the upper sections which otherwise cannot be changed. Limitations of this study were the relatively low resolution of the CBCT scans. A higher resolution would allow to better identify the lateral walls of the nasal cavities or even use of an automated segmentation technique.

Increasing the transverse width of the nasal cavity is commonly considered to also affect the nasal airflow. As the Bernoulli Obstruction Theory states that nasal resistance is inversely proportional to the airspace minimal cross-sectional area and it is widely accepted that there is a correlation between the minimal cross-sectional area and the

airway resistance. However, research though has shown that there only exists a moderate(51-53) or no correlation at all(54-56). Hence the question arises, if the increased effects of the MSE on the nasal cavity are of actual value for the patient and if there is a correlation to breathing. Traditionally, the airway resistance is measured with acoustic rhinometry, where the cross-sectional areas are evaluated perpendicular to the acoustic path. Garcia suggested an improved model to evaluate the nasal resistance by calculating the minimal cross-sectional area perpendicular to the airflow streams with computed fluid dynamics. Multiple airstreams were analyzed and the one with the smallest cross-sectional area was selected for further processing. In this study, he found that a minimal cross-sectional area smaller than 0.37 cm^2, must be present to dominate nasal resistance, which is not expected to occur in healthy subjects, but can occur in severely obstructed cases(57).

Besides nasal resistance, other parameters determine the nasal airflow pattern and Zhao stated that even small anatomical changes can result in significant differences. In a study conducted in 2014, he calculated the fluid dynamics of the nasal cavity before and after resection of the middle turbinate, resulting in a shift of the airflow towards the area of increased volume, decreased airflow speeds and wall shear stress and increased local air pressure(56).

In our study the increase in volume of the airspaces in the nasal cavity were 18.9% higher in the MSE group compared to the Hyrax group. This can be explained by the greater expansion effects on the maxilla and the midface by the miniscrew supported skeletal expander. Nonetheless, one must consider that the air volume in the nasal

cavity is highly affected by the mucosal swelling and follows a circadian rhythm. Additionally, post-expansion edemas might be present and can further reduce the air space. A follow up study at the end of orthodontic treatment might be able to more realistically represent the expansion effects on the air space in the nasal cavity.

Considering the complexity of the airflow within the nasal cavity, a computed fluid dynamics simulation of the treated samples is highly recommended to not only see the changes of the lateral walls of the nasal cavity after MSE expansion but also to better understand the impact of expansion on the nasal airflow and if this can lead to improved breathing. Just increasing the nasal cavity transvers dimensions or increasing the volume does not give any information about the actual effects on the airflow itself.

Conclusion

1) This study utilized a new protocol to evaluate the movement pattern of the lateral walls of the nasal cavity after expansion treatment. Introduction of automated superimposition on the cranial base and reference planes allowed to reliable evaluate bone changes before and after expansion treatment.
2) CBCT images before and immediately after expansion allowed to compare the direct effects of the therapy on the nasal cavity minimizing the effect of other factors, such as bone remodeling, orthodontic treatment effects or growth. A second follow-up time point might be helpful to realistically represent the changes of the nasal cavity air space after expansion induced edemas might be resolved.

3) The MSE appliance showed to produce a similar movement pattern as the Hyrax group in the nasal floor, but did not follow the same pattern at the palatal level. The lateral walls of the nasal cavity do not simply rotate with the maxilla, but bend around dense bone areas like the orbital rims. In the most upper section, the expansion pattern demonstrated to be V-shaped, with little effects close to the cranial base and larger effects at the nasal bone.
4) The expansion effect in the Hyrax group only affected the lower nasal cavity, while MSE produced significantly great expansion effects at any measurement point. MSE treatment effects were measureable at all measurement points, though clinically insignificant at the cranial base level.
5) Further studies could be designed, to evaluate the effects of mini-implant supported expander on the actual airflow in the nasal cavity.
6) Limitations of this study include the relatively low resolution of the CBCT scans. Also, the age groups of the samples should be matched better and even though the statistics suggest sufficient sample size, equal sample sizes would be desirable. Other limitations include the volume calculation of the airspace in the nasal cavity. To reduce the potential side effects of the mucosal swelling application of corticosteroid sprays before CBCT acquisition might be useful.

Appendix Materials

IRB approved by the University of California, Los Angeles.

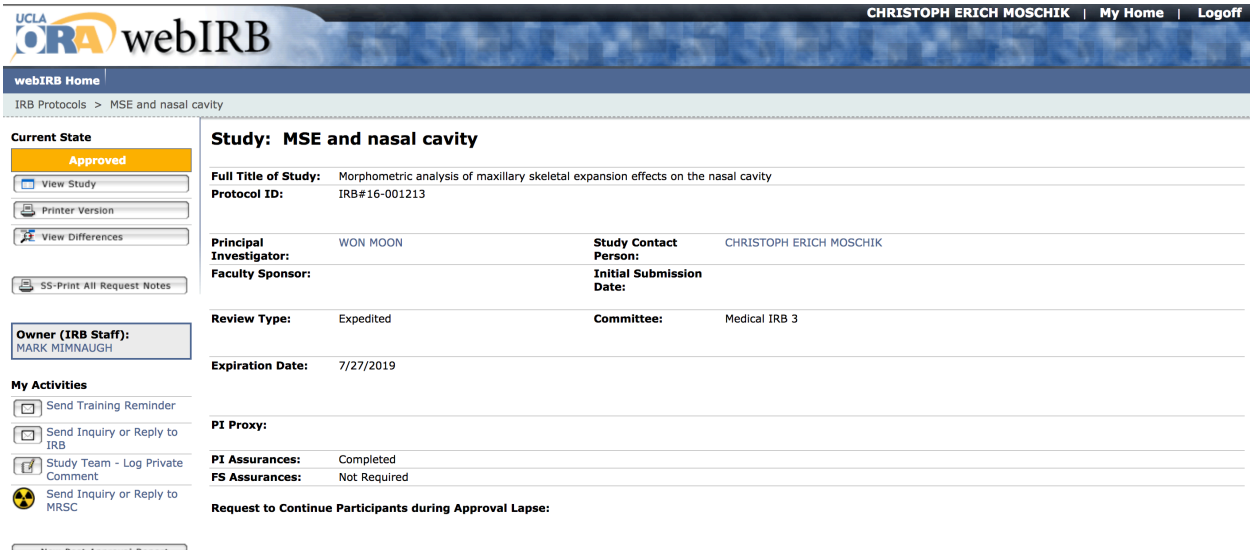

UCLA ORA webIRB

CHRISTOPH ERICH MOSCHIK | My Home | Logoff

webIRB Home

IRB Protocols > MSE and nasal cavity

Current State

Approved

View Study

Printer Version

View Differences

SS-Print All Request Notes

Owner (IRB Staff):
MARK MIMNAUGH

My Activities

Send Training Reminder

Send Inquiry or Reply to IRB

Study Team - Log Private Comment

Send Inquiry or Reply to MRSC

Study: MSE and nasal cavity

Full Title of Study:	Morphometric analysis of maxillary skeletal expansion effects on the nasal cavity		
Protocol ID:	IRB#16-001213		
Principal Investigator:	WON MOON	**Study Contact Person:**	CHRISTOPH ERICH MOSCHIK
Faculty Sponsor:		**Initial Submission Date:**	
Review Type:	Expedited	**Committee:**	Medical IRB 3
Expiration Date:	7/27/2019		
PI Proxy:			
PI Assurances:	Completed		
FS Assurances:	Not Required		

Request to Continue Participants during Approval Lapse:

References

1. Cosmos DAD, 1860. Treatment of irregularity of the permanent or adult teeth. ci.nii.ac.jp

.

2. Cosmos CGD, 1893. Separation of the superior maxilla at the symphysis.

3. Koudstaal MJ, Poort LJ, van der Wal KGH, Wolvius EB, Prahl-Andersen B, Schulten AJM. Surgically assisted rapid maxillary expansion (SARME): a review of the literature. Int J Oral Maxillofac Surg. 2005 Oct;34(7):709–14.

4. Haas AJ. The Treatment Of Maxillary Deficiency By Opening The Midpalatal Suture. http://dxdoiorg/101043/0003-3219(1965)035<0200:TTOMDB>20CO;2. 1965 Jul 15.

5. Persson M, Thilander B. Palatal suture closure in man from 15 to 35 years of age. Am J Orthod. 1977 Jul;72(1):42–52.

6. Melsen B. Palatal growth studied on human autopsy material. A histologic microradiographic study. Am J Orthod. 1975 Jul;68(1):42–54.

7. Woller JL, Kim KB, Behrents RG, Buschang PH. An assessment of the maxilla after rapid maxillary expansion using cone beam computed tomography in growing children. Dental Press J Orthod. 3rd ed. 2014 Jan;19(1):26–35.

8. Timms DJ. A study of basal movement with rapid maxillary expansion. Am J Orthod. 1980 May;77(5):500–7.

9. Garrett BJ, Caruso JM, Rungcharassaeng K, Farrage JR, Kim JS, Taylor GD. Skeletal effects to the maxilla after rapid maxillary expansion assessed with cone-beam computed tomography. American Journal of Orthodontics and Dentofacial Orthopedics. 2008 Jul;134(1):8.e1–8.e11.

10. Lione R, Ballanti F, Franchi L, Baccetti T, Cozza P. Treatment and posttreatment skeletal effects of rapid maxillary expansion studied with low-dose computed tomography in growing subjects. Am J Orthod Dentofacial Orthop. 2008 Sep;134(3):389–92.

11. Handelman CS, Wang L, BeGole EA, Haas AJ. Nonsurgical rapid maxillary expansion in adults: report on 47 cases using the Haas expander. Angle Orthod. 2000 Apr;70(2):129–44.

12. Pinto PX, Mommaerts MY, Wreakes G, Jacobs WV. Immediate postexpansion changes following the use of the transpalatal distractor. J Oral Maxillofac Surg.

2001 Sep;59(9):994–1000–discussion1001.

13. LaBlonde B, Vich ML, Edwards P, Kula K, Ghoneima A. Three dimensional evaluation of alveolar bone changes in response to different rapid palatal expansion activation rates. Dental Press J Orthod. Dental Press; 2017 Feb;22(1):89–97.

14. Mommaerts MY. Transpalatal distraction as a method of maxillary expansion. British Journal of Oral and Maxillofacial Surgery. 1999;37(4):268–72.

15. Mohan CN, Araujo EA, Oliver DR, Kim KB. Long-term stability of rapid palatal expansion in the mixed dentition vs the permanent dentition. American Journal of Orthodontics and Dentofacial Orthopedics. American Association of Orthodontists; 2016 Jun 1;149(6):856–62.

16. Bell RA. A review of maxillary expansion in relation to rate of expansion and patient's age. Am J Orthod. 1982 Jan;81(1):32–7.

17. Isaacson RJ, Ingram AH. Forces Produced by Rapid Maxillary Expansion. Angle Orthod. 1964 Oct 1;34(4):261–70.

18. Bell WH, Epker BN. Surgical-orthodontic expansion of the maxilla. Am J Orthod. 1976 Nov;70(5):517–28.

19. Brown G. The surgery of oral and facial diseases and malformations: their diagnosis and treatment including plastic surgical reconstruction. 1938.

20. Bays RA, Greco JM. Surgically assisted rapid palatal expansion: an outpatient technique with long-term stability. J Oral Maxillofac Surg. 1992 Feb;50(2):110–3–discussion114–5.

21. Alpern MC, Yurosko JJ. Rapid palatal expansion in adults with and without surgery. Angle Orthod. 1987 Jul;57(3):245–63.

22. Glassman AS, Nahigian SJ, Medway JM, Aronowitz HI. Conservative surgical orthodontic adult rapid palatal expansion: Sixteen cases. Am J Orthod. 1984;86(3):207–13.

23. Lagravere MO, Carey J, Heo G, Toogood RW, Major PW. Transverse, vertical, and anteroposterior changes from bone-anchored maxillary expansion vs traditional rapid maxillary expansion: A randomized clinical trial. American Journal of Orthodontics and Dentofacial Orthopedics. American Association of Orthodontists; 2010 Mar 1;137(3):304.e1–304.e12.

24. Lee RJ, Moon W, Hong C. Effects of monocortical and bicortical mini-implant anchorage on bone-borne palatal expansion using finite element analysis. American Journal of Orthodontics and Dentofacial Orthopedics. 2017 May;151(5):887–97.

25. Asanza S, Cisneros GJ, Nieberg LG. Comparison of Hyrax and bonded expansion appliances. Angle Orthod. 1997;67(1):15–22.

26. Wilmes B, Panayotidis A, Drescher D. Fracture resistance of orthodontic mini-implants: a biomechanical in vitro study. Eur J Orthod. Oxford University Press; 2011 Aug 1;33(4):396–401.

27. Ludwig B, Glasl B, Bowman SJ, Wilmes B, Kinzinger GSM, Lisson JA. Anatomical guidelines for miniscrew insertion: palatal sites. J Clin Orthod. 2011 Aug;45(8):433–41–quiz467.

28. Petrey JS, Saunders MM, Kluemper GT, Cunningham LL, Beeman CS. Temporary anchorage device insertion variables: effects on retention. Angle Orthod. 2010 Jul;80(4):634–41.

29. Cantarella D, Dominguez-Mompell R, Mallya SM, Moschik C, Pan HC, Miller J, et al. Changes in the midpalatal and pterygopalatine sutures induced by micro-implant-supported skeletal expander, analyzed with a novel 3D method based on CBCT imaging. Prog Orthod. Progress in Orthodontics; 2017 Sep 14;18(1):1–12.

30. Ribeiro ANC, de Paiva JB, Rino-Neto J, Illipronti-Filho E, Trivino T, Fantini SM. Upper airway expansion after rapid maxillary expansion evaluated with cone beam computed tomography. Angle Orthod. 2012 May;82(3):458–63.

31. Palaisa J, Ngan P, Martin C, Razmus T. Use of conventional tomography to evaluate changes in the nasal cavity with rapid palatal expansion. American Journal of Orthodontics and Dentofacial Orthopedics. Elsevier; 2007 Oct;132(4):458–66.

32. Garib DG, Henriques JFC, Janson G, Freitas MR, Coelho RA. Rapid Maxillary Expansion—Tooth Tissue-Borne Versus Tooth-Borne Expanders: A Computed Tomography Evaluation of Dentoskeletal Effects. dx.doi.org. 2009.

33. Haralambidis A, Ari-Demirkaya A, Acar A, Kucukkeles N, Ateş M, Özkaya S. Morphologic changes of the nasal cavity induced by rapid maxillary expansion: a study on 3-dimensional computed tomography models. Am J Orthod Dentofacial Orthop. 2009 Dec;136(6):815–21.

34. Hahn L, Marchioro EM, Rizzato SD, Roithmann R, Costa NPD. Avaliação do volume da cavidade nasal antes e após a expansão rápida da maxila por meio da rinometria acústica. Ortodon gaúch. 1999;3(2):85–96.

35. Babacan H, Sökücü O, Doruk C, Ay S. Rapid maxillary expansion and surgically assisted rapid maxillary expansion effects on nasal volume. Angle Orthod. 2006 Jan;76(1):66–71.

36. Oliveira De Felippe NL, Da Silveira AC, Viana G, Kusnoto B, Smith B, Evans

CA. Relationship between rapid maxillary expansion and nasal cavity size and airway resistance: short- and long-term effects. Am J Orthod Dentofacial Orthop. 2008 Sep;134(3):370–82.

37. Doruk C, Sökücü O, Bicakci AA, Yilmaz U, Taş F. Comparison of nasal volume changes during rapid maxillary expansion using acoustic rhinometry and computed tomography. Eur J Orthod. The Oxford University Press; 2007 Jun 1;29(3):251–5.

38. Yushkevich PA, Piven J, Hazlett HC, Smith RG, Ho S, Gee JC, et al. User-guided 3D active contour segmentation of anatomical structures: Significantly improved efficiency and reliability. NeuroImage. 2006 Jul;31(3):1116–28.

39. Mozzo P, Procacci C, Tacconi A, Martini PT, Andreis IAB. A new volumetric CT machine for dental imaging based on the cone-beam technique: preliminary results. Eur Radiol. Springer-Verlag; 1998 Nov 23;8(9):1558–64.

40. Gribel BF, Gribel MN, Frazäo DC, McNamara JA, Manzi FR. Accuracy and reliability of craniometric measurements on lateral cephalometry and 3D measurements on CBCT scans. Angle Orthod. 2011 Jan;81(1):26–35.

41. Hatcher DC, Aboudara CL. Diagnosis goes digital. American Journal of Orthodontics and Dentofacial Orthopedics. 2004 Apr;125(4):512–5.

42. Björk A. Sutural growth of the upper face studied by the implant method. Eur J Orthod. 2007 Apr 1;29(Supplement 1):i82–8.

43. Doppel DM, Damon WM, Joondeph DR, Little RM. An investigation of maxillary superimposition techniques using metallic implants. American Journal of Orthodontics and Dentofacial Orthopedics. 1994 Feb;105(2):161–8.

44. Weissheimer A, Menezes LM, Koerich L, Pham J, Cevidanes LHS. Fast three-dimensional superimposition of cone beam computed tomography for orthopaedics and orthognathic surgery evaluation. Int J Oral Maxillofac Surg. Elsevier; 2015 Sep 1;44(9):1188–96.

45. Cevidanes LHC, Heymann G, Cornelis MA, DeClerck HJ, Tulloch JFC. Superimposition of 3-dimensional cone-beam computed tomography models of growing patients. American Journal of Orthodontics and Dentofacial Orthopedics. 2009 Jul;136(1):94–9.

46. Cevidanes LHS, Styner MA, Proffit WR. Image analysis and superimposition of 3-dimensional cone-beam computed tomography models. American Journal of Orthodontics and Dentofacial Orthopedics. 2006 May;129(5):611–8.

47. Cevidanes L, Baccetti T, Franchi L, McNamara JA, De Clerck H. Comparison of two protocols for maxillary protraction: bone anchors versus face mask with rapid maxillary expansion. Angle Orthod. 2010 Aug 31;80(5):799–806.

48. Wertz RA. Skeletal and dental changes accompanying rapid midpalatal suture opening. Am J Orthod. 1970;58(1):41–66.

49. MacGinnis M, Chu H, Youssef G, Wu KW, Machado AW, Moon W. The effects of micro-implant assisted rapid palatal expansion (MARPE) on the nasomaxillary complex--a finite element method (FEM) analysis. Prog Orthod. Springer Berlin Heidelberg; 2014 Aug 29;15(1):52.

50. Lee RJ, Moon W, Hong C. Effects of monocortical and bicortical mini-implant anchorage on bone-borne palatal expansion using finite element analysis. Am J Orthod Dentofacial Orthop. 2017 May;151(5):887–97.

51. Scadding GK, Darby YC, Austin CE. Acoustic rhinometry compared with anterior rhinomanometry in the assessment of the response to nasal allergen challenge. Clin Otolaryngol Allied Sci. 1994 Oct;19(5):451–4.

52. Tai CF, Ho KY, Hasegawa M. Evaluating the sensation of nasal obstruction with acoustic rhinometry and rhinomanometry. Kaohsiung J Med Sci. 1998 Sep;14(9):548–53.

53. Wandalsen GF, Mendes AI, Solé D. Correlation between nasal resistance and different acoustic rhinometry parameters in children and adolescents with and without allergic rhinitis. Braz J Otorhinolaryngol. 2012 Dec;78(6):81–6.

54. Naito K, Miyata S, Saito S, Sakurai K, Takeuchi K. Comparison of perceptional nasal obstruction with rhinomanometric and acoustic rhinometric assessment. European Archives of Oto-Rhino-Laryngology. Springer-Verlag; 2001;258(10):505–8.

55. Numminen J, Ahtinen M, Huhtala H, Laranne J, Rautiainen M. Correlation between rhinometric measurement methods in healthy young adults. American Journal of Rhinology. 2002 Jul;16(4):203–8.

56. Zhao K, Malhotra P, Rosen D, Dalton P, Pribitkin EA. Computational fluid dynamics as surgical planning tool: a pilot study on middle turbinate resection. Van Valkenburgh B, Smith T, Craven B, Laitman JT, editors. Anat Rec (Hoboken). 2014 Nov;297(11):2187–95.

57. Garcia GJM, Hariri BM, Patel RG, Rhee JS. The relationship between nasal resistance to airflow and the airspace minimal cross-sectional area. J Biomech. 2016 Jun;49(9):1670–8.